

FAMU/FSU College of Engineering



Department of Mechanical Engineering

Sponsors:



Mentor:

Dr. Rajan Kumar

Fall Final Report

Team 24: Intercollegiate Rocket Engineering Competition

December 5, 2016

Names:	Tariq Grant	Contact Email:	twg13@my.fsu.edu
	William Pohle		wjp14c@my.fsu.edu
	Brandon Gusto		blg13@my.fsu.edu
	Alexandra Mire		aem12d@my.fsu.edu

Contents

List of Figures	vi
List of Tables	vii
Abstract	viii
Acknowledgements	ix
1 Introduction	1
2 Background and Literature Review	1
2.1 Early History	1
2.2 Modern Sounding Rockets	1
2.3 Sounding Rocket Composition	2
3 Project Details	2
3.1 Needs Statement	2
3.2 Goal Statement and Objectives	2
3.3 Constraints	3
3.3.1 Vehicle & Payload Requirements	3
3.3.2 General Requirements	3
4 Project Scope	4
5 Methodology	5
5.1 Safety and Logistics	5
5.2 Launch Vehicle	5
5.3 Verification	6
5.4 Expected Results	7
6 Vehicle Development	7
6.1 System Overview	7
6.2 Flight Model	8
6.3 Propulsion	10
6.4 Nose Cone Shape Optimization	12
6.5 Airframe Material Selection	13
6.5.1 Aluminum 6061	14
6.5.2 High Modulus Carbon Fibre	15
6.5.3 Fiberglass	16
6.5.4 Selection	17

6.6	Stability	17
6.7	Recovery Systems	18
6.7.1	Parachute System	18
6.7.2	Deployment System	21
6.8	Avionics	23
6.9	Payload Design	23
7	Final Vehicle Specifications	25
7.1	Launch Vehicle Overview	25
7.2	Booster	26
7.3	Drogue Parachute Section	28
7.4	Avionics Bay	29
7.5	Main Parachute Section	31
7.6	Nose Cone and Payload Bay	31
7.7	Cost Analysis	33
8	Launch Vehicle Validation	33
8.1	Structural Integrity Analysis	33
8.1.1	Solid Mechanics	34
8.1.1.1	Assumptions	34
8.1.1.2	COMSOL Models of Simple Rocket Tube	35
8.1.1.3	COMSOL Models of Rocket Tube and Motor Housing	36
8.1.1.4	Verification and Validation	37
8.2	Flight Performance Simulation	38
8.2.1	In-House Simulation	38
8.2.2	OpenRocket	40
8.3	Failure Analysis	42
9	Project Planning	43
9.1	Background Research and Concept Generation	44
9.2	Detailed Design and Analysis	44
9.3	Design Implementation	44
9.4	Test and Revise	45
9.5	Safety and Risks	45
9.6	Competition Deadlines	46
9.7	Cost of Participation	47
10	Conclusion	47
	References	49

Appendix	50
Biography	63

Table of Figures

Figure 1:	House of Quality comparing engineering values with the requirements.	6
Figure 2:	Rocket subsystems.[4]	8
Figure 3:	Flight apogees based on mass of rocket for four solid rocket motors.	10
Figure 4:	Maximum theoretical mach number based on mass of the rocket for the four different motors analyzed.	11
Figure 5:	Nose cone profile as a function of mach number.[5]	12
Figure 6:	Stress vs slenderness ratio curve showing regions of safety known as Euler and Johnson regions.	14
Figure 7:	Plot of buckling factor of safety and apogee versus increasing tube thickness.	15
Figure 8:	Plot of buckling factor of safety and apogee versus increasing tube thickness using carbon fibre.	16
Figure 9:	Plot of buckling factor of safety and apogee versus increasing tube thickness using fiberglass.	17
Figure 10:	A dual deployment parachute system after deployment.	19
Figure 11:	A large-scale reefed parachute system after deployment, still in its reefed stage.	19
Figure 12:	A steerable parafoil guiding an experimental flight vehicle.	20
Figure 13:	Pugh Selection Matrix for Recovery System showing that with the selected engineering characteristics, the reefed parachute narrowly scores more points than the baseline.	20
Figure 14:	Exploded view of the Peregrine compressed CO ₂ ejection system.	21
Figure 15:	A simple diagram of a rocket motor with the gas generator on the left side at the forward end of the motor.	22
Figure 16:	Rocketman 3ft Parachute and B2 XXL parachute contained in the main parachute and drogue parachute bays.	22
Figure 17:	Flow injectors modify the stall characteristics of an experimental aircraft.	24
Figure 18:	Comparison of standard cubesat frames.	24
Figure 19:	View 1 of the final launch vehicle.	25
Figure 20:	View 2 of the final launch vehicle.	25
Figure 21:	The 5 main rocket sections in order of assembly.	26
Figure 22:	Detailed view of the rocket motor casing, thrust structure, stabilization fins, and housing tube.	27
Figure 23:	Detailed view of the main centering ring.	27

Figure 24:	The drogue bay shown immediately following the booster section. In this section the parachute is represented by a brown cylinder and the kevlar shock cord is not shown to increase view-ability.	28
Figure 25:	The avionics bay enclosed.	29
Figure 26:	The avionics bay opened.	30
Figure 27:	The main parachute bay shown immediately following the avionics bay. In this section the parachute is represented by a brown cylinder and the kevlar shock cord is not shown to increase view-ability.	31
Figure 28:	The payload will be housed inside of the nose cone and attached tube section.	32
Figure 29:	The nose cone with the payload section and centering ring.	32
Figure 30:	Thrust curve of the CTI 9955M1450 high power rocket motor [14]	34
Figure 31:	2D COMSOL models of a simple rocket tube	36
Figure 32:	3D COMSOL models of a simple rocket tube	36
Figure 33:	2D COMSOL models of rocket tube and housing	37
Figure 34:	3D COMSOL models of rocket tube and housing	37
Figure 35:	Plot of the height of the rocket AGL during the ascent phase of the flight.	39
Figure 36:	Plot of the mach number of the rocket during the motor burn.	40
Figure 37:	2D and 3D graphics of the rocket design in OpenRocket.	41
Figure 38:	The distance of the center of gravity from the nose of the rocket during flight.	42
Figure 39:	Failure Modes and Effects Analysis.	43
Figure 40:	House of Quality comparing Engineering Values with Requirements	50
Figure 41:	Rocket Subsystems.[4]	51
Figure 42:	Flight apogees based on mass of rocket for four solid rocket motors.	51
Figure 43:	Maximum theoretical mach number based on mass of the rocket for the four different motors analyzed.	52
Figure 44:	The distance of the center of gravity from the nose of the rocket during flight.	52
Figure 45:	Nose cone profile as a function of mach number.[5]	53
Figure 46:	Plot of buckling factor of safety and apogee versus increasing tube thickness.	54
Figure 47:	Plot of buckling factor of safety and apogee versus increasing tube thickness using carbon fibre.	55
Figure 48:	Plot of buckling factor of safety and apogee versus increasing tube thickness using fiberglass.	56
Figure 49:	Pugh Selection Matrix for Recovery System	57

Figure 50:	Plot of the height of the rocket AGL during the ascent phase of the flight.	58
Figure 51:	Plot of the mach number of the rocket during the motor burn.	59
Figure 52:	Gantt Chart for Fall 2016	59
Figure 53:	Gantt Chart for Competition Deadlines	62

Table of Tables

Table 1:	List of assumptions in the model.	9
Table 2:	Combinations of Mach number and weight for a 10,000 ft apogee.	11
Table 3:	Standard CubeSat dimensions that the payload components must fit within.	24
Table 4:	Overview of launch vehicle subsystem decisions.	26
Table 5:	Cost breakdown of rocket into the 5 main sections.	33
Table 6:	Material Properties Used [16]	35
Table 7:	Comparison of data from the in-house simulation and OpenRocket.	41
Table 8:	Bill of materials to be ordered at the end of the fall semester.	45
Table 9:	Cost breakdown of participating in the competition	47
Table 10:	Booster Section Cost. Each component is listed by its location within the section from bottom to top.	60
Table 11:	Drogue Section Cost. Each component is listed by its location within the section from bottom to top.	60
Table 12:	Avionics Bay Cost. Each component is listed by its location within the section from bottom to top.	61
Table 13:	Main Parachute Bay Cost. Each component is listed by its location within the section from bottom to top.	61
Table 14:	Nose Cone section Cost. Each component is listed by its location within the section from bottom to top.	61

Abstract

Team 24 of the 2016-2017 Senior Design class has committed to designing and building a competitive rocket for the Experimental Sounding Rocket Association's Intercollegiate Rocket Engineering Competition (IREC). This competition requires that a sounding rocket be designed, built, and flown to 10,000 ft above ground level; and be safely recovered. For this purpose, we have determined that a rocket with fixed fins and composed of fiberglass, should be created. Housed inside of this should be two recovery systems, our payload and our flight computer. This should all be propelled by a solid grain rocket motor and the delayed black powder gas generator should be used for our recovery system with a CO₂ canister as a backup. Testing shall be done via a scale model and eventually flight testing of our system. Once all things have been deemed satisfactory, Team 24 will participate in the IREC held at Spaceport America.

Acknowledgements

Team 24 would like to acknowledge the different people and organizations that have assisted throughout this venture:

Firstly, this team would like to thank Dr. Rajan Kumar for his assistance in developing concepts for the research experiment to fly on our rocket. We would also like to thank John Hansel for introducing the team to a number of launch and safety procedures specified by the NAR and Tripoli rocket organizations. Additionally, Team 24 would like to express our appreciation of Dr. Nikhil Gupta and Dr. Chiang Shih for oversight and advisement of the senior design projects.

1. Introduction

The Experimental Sounding Rocket Association (ESRA) annually hosts the Intercollegiate Rocket Engineering Competition (IREC). This competition requires teams from over a dozen universities to design, build, and launch experimental sounding rockets. A key point of the competition is that the vehicles must carry a payload which performs a scientific experiment.

It is the goal of Team 24 to compete in this competition and create a rocket capable of reaching an apogee of 10,000 ft above ground level (AGL), while simultaneously performing a useful scientific experiment. Team 24 aims to conduct all activities as safely and professionally as possible, while delivering a vehicle with truly outstanding performance.

2. Background and Literature Review

2.1 Early History

Experimental rocketry can be traced back to 1806, when Claude Ruggieri created rockets to carry animals into the atmosphere. However, sounding rockets in their current use and configuration can be attributed to a Russian rocketry pioneer by the name of Mikhail Tikhonoravov. In 1933, Tikhonoravov launched a liquid fueled rocket carrying scientific instrumentation [1]. Later in 1946, the V2 rocket, famous for causing devastation during the second World War, was used by both American and Russian scientists for atmospheric experimentation [2].

Use of sounding rockets exploded during the International Geophysical Year, from 1957 to 1958. During this period approximately 200 rockets were launched. Upper atmospheric and space experiments were being performed at a rapid rate. Some notable activities during this time frame include the launching of the first probes to the moon, along with the discoveries of the Van Allen belts and the magnetosphere [1] [2].

2.2 Modern Sounding Rockets

Currently, sub-orbital sounding rockets are used world-wide for a vast expanse of disciplines and studies. There are several reasons for this, but the most compelling is their large range of testing altitude. Weather balloons are primarily limited by their speed and their maximum altitude of roughly 120,000 ft. Satellites in orbit around the Earth operate in the vacuum of space and cannot study atmospheric phenomenon directly. Thus,

sounding rockets deliver a unique capability to do direct atmospheric measurements at high altitudes and at very high mach numbers. [1]

2.3 Sounding Rocket Composition

A series of subsystems composes the sub-orbital sounding rocket: the payload, recovery system, flight control system, propulsion system and telemetry system. All of these systems possess unique hardware, however, of most interest to this project is the payload. This system is typically housed inside of the nose cone. As such, the payload can be separated from the launch vehicle, allowing for it to be used multiple times for different experiments. [3].

3. Project Details

3.1 Needs Statement

This team's objective is to design and develop a recoverable rocket that safely delivers a payload to an apogee of 10,000 ft AGL. The payload needs to have a scientific or engineering purpose, and every component must be recoverable. Additionally, the rocket and payload should conform to the rules of the Experimental Sounding Rocket Association's 2017 Intercollegiate Rocket Engineering Competition.

3.2 Goal Statement and Objectives

Successfully design, build, and fly a vertical take-off, single-stage, rocket powered launch vehicle to an apogee of 10,000 ft AGL, and deploy a scientifically useful payload as part of the Intercollegiate Rocket Engineering Competition sponsored by the Experimental Sounding Rocket Association.

In order to accomplish this goal, the following objectives are set by our team:

- Brainstorm concepts for launch vehicle and for payloads that may be useful to the scientific or engineering community
- Conduct substantial background research into launch vehicle aerodynamics, materials, controls, and structural mechanics
- Benchmark the rocket-payload system using previous competition entries as case studies

- Develop a set of engineering characteristics using engineering parameters, design variables, and constraints
- Utilize engineering tools such as a house of quality chart to select parts and materials that best meet our goal
- Develop scale prototype to validate initial engineering design
- Reiterate on prototype to improve performance
- Design, fabricate, and assemble necessary parts for both test and flight articles
- Develop flight software and integrate into avionics sensors to control rocket functions
- Conduct flight testing of recovery system and flight controller
- Compete at the IREC

3.3 Constraints

The Basic Category of the Intercollegiate Rocket Engineering Competition has a set of rules and requirements pertaining to the design of the vehicle and its payload. In addition there are numerous safety requirements imposed for the launch of the vehicle.

3.3.1 Vehicle & Payload Requirements

- The vehicle must attain an altitude of 10,000 ft AGL
- The payload must be at least 8.8 lbs
- The vehicle and payload must be recoverable
- The payload must not be used to alter the stability of the rocket
- The vehicle must have an altimeter and record data using a flight computer
- A maximum of one propulsive stage is allowed
- Propulsion must use non-toxic fuels
- Payload may not contain hazardous materials or live animals

3.3.2 General Requirements

In addition to the rules regarding the design of the vehicle and payload, several other rules should be observed regarding the flight and launch preparation.

- The vehicle must be able to return to a safe-mode after arming
- The vehicle should attain a speed of 100 ft/s before leaving the launch rail
- The vehicle and payload must have a recovery system
- Main parachute should slow rocket to at least 30 ft/s by 1,500 ft AGL

4. Project Scope

The sounding rocket developed through the course of this project should fulfill the competition requirements imposed by the IREC. Additionally, the research payload should provide useful data for researchers at the FAMU-FSU College of Engineering. Nearly all components of the rocket shall be recoverable and reusable for any subsequent flights, if additional experimental flights are desired.

A number of elements of the launch vehicle can be purchased, however the body, fins, nose cone, software, and experimental payload will require design, development, and some components may require in-house manufacturing. Our major purchases will be the rocket motors required for test flights and validation.

As per the IREC evaluation criteria, the launch vehicle produced by Team 24 will be evaluated based upon the altitude the rocket is capable of reaching as well as the damage levels to components during flight. Our vehicle development process will be completed when, following a thorough test flight program, (1) the rocket consistently reaches the target altitude, and (2) all components are recovered without damage. Beyond that point, group resources will largely be dedicated to optimizing the data obtained through the experimental payload of the rocket, which will be evaluated based upon the quality and accuracy of the data obtained.

In June of 2017 the team will travel to participate in the Intercollegiate Rocket Engineering Competition held at Spaceport America and hosted by the Experimental Sounding Rocket Association. It is our aim to place highly at this competition and bring further prestige to our university.

Finally, it is the hope of Team 24 that successful participation in the Intercollegiate Rocket Engineering Competition will result in an increased level of enthusiasm and usher forth a wave of interest in rocketry and spaceflight at the FAMU-FSU College of Engineering. We sincerely hope that this project will become a yearly venture for the College of Engineering and that, in later years, more advanced vehicles can be developed and entered into competitions.

5. Methodology

To accomplish the previously stated goals and objectives, the design team has envisioned a methodology to be adhered to in all aspects of the design process. These methodologies are described in detail in the following sections.

5.1 Safety and Logistics

- Comply with legal requirements associated with high power rocketry and the Intercollegiate Rocket Engineering Competition
- Develop risk assessment and safety plan to ensure safety of design team and reduce liability risks
- Perform certification tests and attain rocketry organization membership to ensure launch site access and high-power motor access

5.2 Launch Vehicle

Before beginning the main launch vehicle design, the features that would be most important to focus on were determined. This was done by defining the characteristics of sounding rockets, as shown below.

- Stability : The ability of the rocket to maintain a straight flight path
- Rocket Weight : The amount of mass that the rocket motor would be required to lift
- Total Impulse : The culmination of the burn time and force output of the motor selected
- Reliability : The probability that the components will perform as designed
- Scientific Value : The usefulness of the experiment being performed
- Material Strength : The ability of the material to withstand the forces it will be subject to
- Avionics : The flight controller and sensor package

By weighting the correlation between these features and the competition requirements and constraints, the following table was produced.

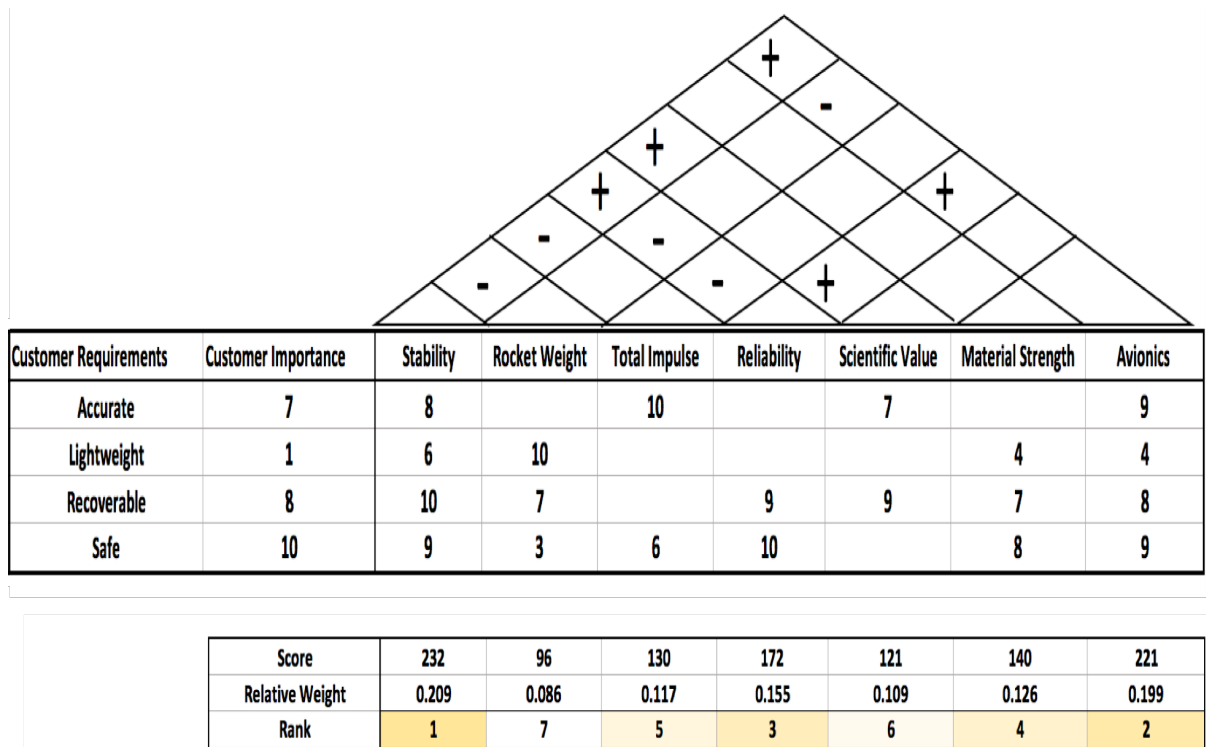


Figure 1: House of Quality comparing engineering values with the requirements.

The House of Quality implies that, in order to produce a competitive vehicle, the most critical aspects of the design are stability, avionics, and reliability. With the ranking of characteristics performed, the actual design can be completed according to the following steps:

1. Develop a mathematical model to simulate the flight profile of the vehicle
2. Select a rocket motor to determine target vehicle weight
3. Select vehicle outer mold material
4. Determine aerodynamic shape, fin geometry, and other parameters related to flight stability
5. Determine internal components for recovery, payload and avionics systems
6. Determine if the final design meets the necessary performance and safety specifications; if not, return to step 1 and make adjustments.

5.3 Verification

A number of tests are to be conducted by the design team to ensure that the final design meets each and every criteria across the board. The proceedings for each of the following

tests will be outlined in the safety plan and risk assessment. These tests will be scheduled and performed under the appropriate supervision at predetermined locations. All test results will be documented and any discrepancies will be reported to the advisory staff.

- Payload Test : The payload will be tested for functionality
- Aerodynamic Drag test : Perform sub-scale wind test on model of launch vehicle to verify flight characteristics
- Recovery Test : Test parachute deployment systems for reliability with ground and flight tests
- Flight Test : Test the fully integrated, final design for functionality

5.4 Expected Results

At the end point of this project, it is expected that a competitive rocket capable of carrying an 8.8 lbs payload will be created by Team 24. In addition to this, Team 24 expects to launch this rocket at the ESRA's IREC competition in 2017. For the purposes of Senior Design, there are also other expectations.

The results of this project will amount to a number of deliverables:

- All documentation pertaining to the Senior Design curriculum
- All documentation pertaining to the ESRA IREC rules and regulations
- All documentation pertaining to NAR and Tripoli rocket certification
- Final flight hardware to be flown in competition
- Final poster for Senior Design

6. Vehicle Development

The development of a sounding rocket requires an understanding of a multitude of engineering facets.

6.1 System Overview

The launch vehicle is composed of several subsystems. The figure below details the approximate layout of our launch vehicle[4]. As can be seen in the figure, the payload will be housed in the nose cone. Aft of the nose cone is the main parachute. Followed by

the main parachute is avionics bay. This includes all flight computers and sensing devices. Aft of the avionics bay is the drogue parachute, which will be released before the main parachute. Finally, the motor will be housed at the rear of the rocket and surrounding it will be the stabilization fins.

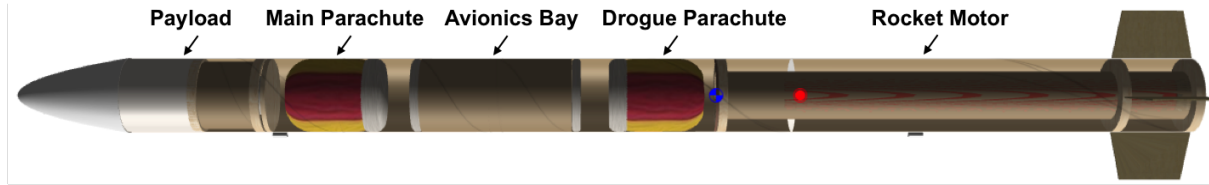


Figure 2: Rocket subsystems.[4]

6.2 Flight Model

Before a clean-sheet design of a rocket can be started, a simplified model must be created to describe the flight of the vehicle. The model must take into account the forces and varying parameters that affect the vehicle during the flight. This is necessary to determine the type of motor needed; specifically its necessary thrust profile and total impulse can be estimated. From this, an estimate of the maximum weight of the vehicle systems can be made and thus many elements of the vehicle can be decided.

A model was created which uses Newton's Laws and the classical equations of motion iteratively to simulate the trajectory of the rocket up to the point of apogee. The basis of the code is Newton's second law,

$$F = \frac{dp}{dt} = \frac{d(mv)}{dt}. \quad (1)$$

Given that the mass of the vehicle is changing constantly due to the loss of propellant, the previous Equation (1) would be unwieldy to use in practice. However, by taking finite (sufficiently small) time steps $dt \approx \Delta t$, the mass can be assumed to be constant within each interval without much loss of accuracy. Then (1) becomes

$$F_i = m_i a_i, \quad (2)$$

which is a more familiar and manageable form. Then separating each component of the vehicle by its mass, namely the fixed-mass motor casing, the fixed weight associated with the airframe and internal components, and the variable mass of the propellants, the model represents the total mass as

$$m_{\text{tot}_i} = m_{\text{fixed}} + m_{\text{propellant}_i}. \quad (3)$$

Then given the initial conditions of the vehicle before launch, the acceleration, velocity and position at each time step can be determined. This is done using

$$a_i = \frac{F_{\text{tot}_i}}{m_{\text{tot}_i}} \quad (4)$$

$$v_{i+1} = v_i + a_i \Delta t \quad (5)$$

$$r_{i+1} = r_i + v_i \Delta t + \frac{1}{2} a_i (\Delta t)^2. \quad (6)$$

While these simple equations form the basis of the model, the determination of the total force on the rocket at each time step is the most exacting part of the model. Summarized in the table below is a list of assumptions that the model makes in order to estimate the total force on and mass of the vehicle at each time step.

Term	Equation	Explanation
ρ	$\rho = \rho_0 \exp(-r/r_0)$	The sea-level air density is ρ_0 and r is present altitude while r_0 is maximum atmospheric altitude
F_{thrust}	Empirical	For each rocket motor analyzed, the thrust profile data is used at each time step during the burn
F_{form}	$F_{\text{form}} = \frac{1}{2} C_d \rho A_{\text{front}} v^2$	Standard equation for form drag on a bluff body
F_{friction}	$F_{\text{friction}} = \frac{1}{2} C_f \rho A_{\text{wetted}} v^2$	Standard equation for drag caused by friction of the air moving over the vehicle surface
C_f	$C_f = (1.5 \log \text{Re} - 5.6)^{-2}$	Empirical relationship used to estimate the coefficient of skin friction for a body in turbulent flow
$m_{\text{propellant}}$	$m_{\text{propellant}} = m_{\text{prop init}} - b \Delta t$	Letting b be a constant burn rate of the propellant, this model assumes the loss of propellant mass is linear

Table 1: List of assumptions in the model.

The code developed using this model takes in performance data from commercial rocket motors, an arbitrary fixed mass (not including the motor casing), and information about the dimensions of the motor in order to determine the minimum diameter of the vehicle's airframe. The output of the program is information about each motor's overall performance as well as the forces acting on the vehicle during the flight, which is important for other design aspects.

6.3 Propulsion

The simulation that was developed has the ability to predict the trajectory of the rocket throughout the entire flight; from liftoff, burnout, coast phase and finally apogee. Since one of the main criteria in designing the vehicle is mass, it is important to know how much a particular motor can lift to the target altitude. In order to determine what the maximum fixed airframe mass could be, the simulations were run with a locus of potential masses. As can be seen in Figure (42), four of the most suitable motors were analyzed for a range of potential masses. Their predicted apogees are plotted along the ordinate. Following the intersection of the target altitude of 10,000 ft and each curve downward, it is clear what the target weight of the airframe should be for each particular motor.

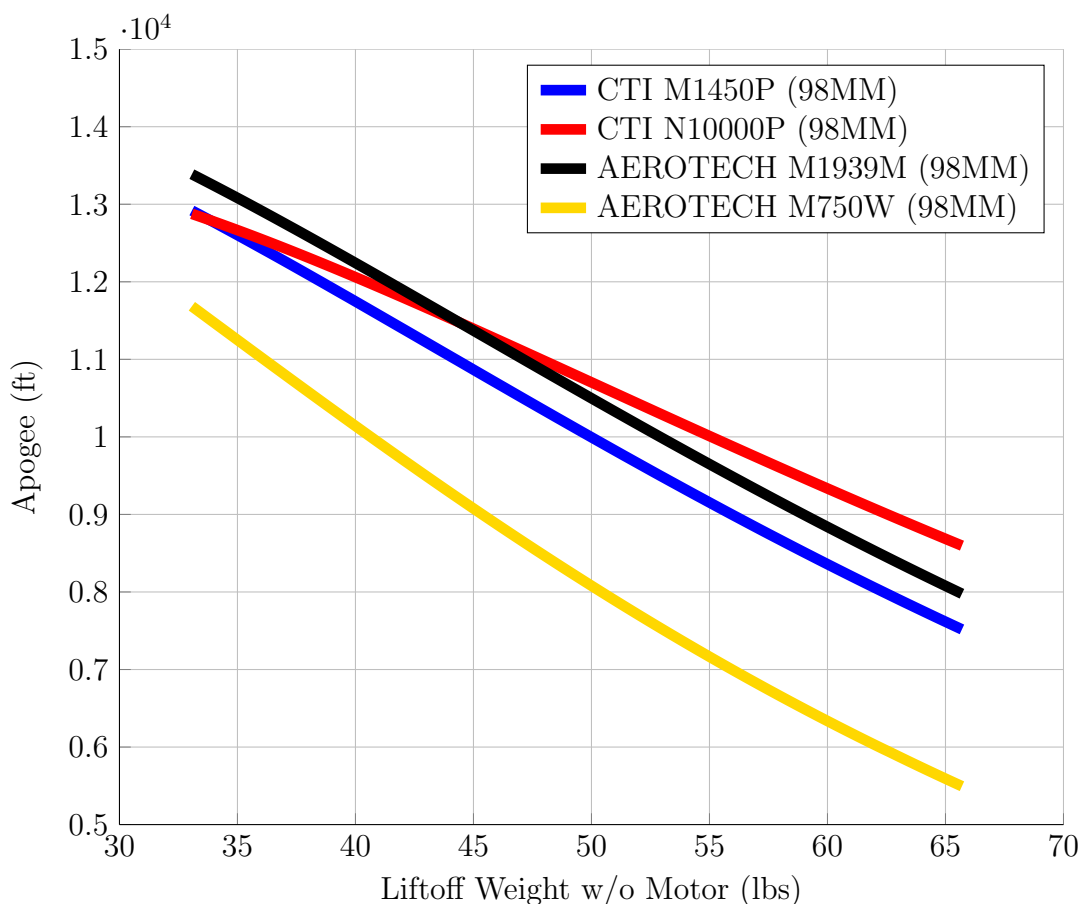


Figure 3: Flight apogees based on mass of rocket for four solid rocket motors.

Since the code calculates the entire trajectory, the simulation also has the added functionality of calculating the maximum theoretical Mach number encountered by the vehicle. These results are shown in Figure (51). By combining the information from Figure(42) with that of Figure (51), Table (2) details the expected Mach number for weights which allow a 10,000 ft apogee.

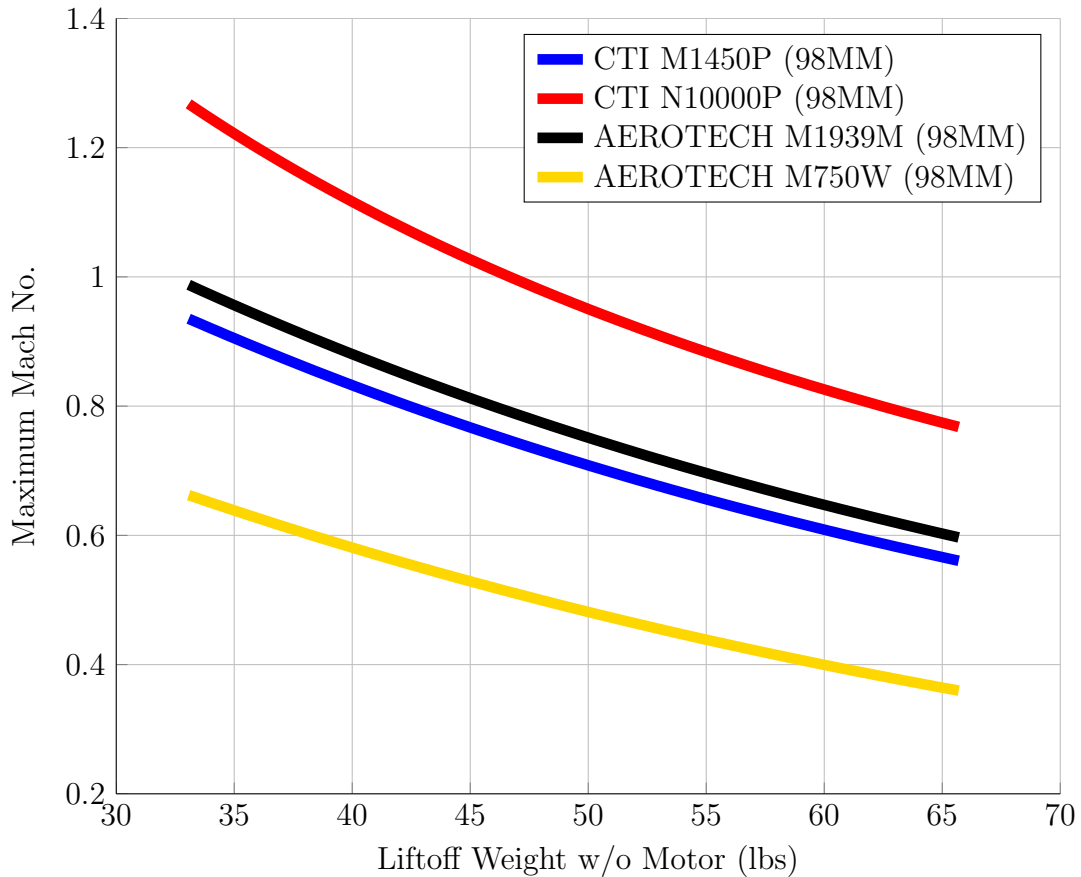


Figure 4: Maximum theoretical mach number based on mass of the rocket for the four different motors analyzed.

From Table (2) it can be seen that, by utilizing any one of the four motors, the rocket will be moving in the range of Mach 0.5 to Mach 0.9.

Motor	Mach Number	Liftoff Weight w/o Motor
M750W	0.57	40.5 lbs
M1450P	0.71	49.8 lbs
M1939W	0.72	52.9 lbs
N10000P	0.89	54.9 lbs

Table 2: Combinations of Mach number and weight for a 10,000 ft apogee.

The motor that gives the best design margins, allowing heavier and less expensive materials, is the N10000P motor from Cesaroni Technology Incorporated. Lower expense motors with sufficient capability include the M1450P and M1939W.

6.4 Nose Cone Shape Optimization

Nose cone design is influenced greatly by the intended speed of the moving body. For subsonic flights, domal shaped rocket noses have lower drag characteristics than cone shaped noses. The opposite is true once the rocket enters the supersonic regime. Since our rocket will be moving at a subsonic velocity, a domal shape is desired.

Extensive research has been done on this subject, and the following figure details the ideal shapes for given mach numbers based on empirical data. By following the information presented in "The Descriptive Geometry of Nose Cones," [5] it was determined that the simplest and most effective cone shape would have a profile proportional to $x^{0.5}$.

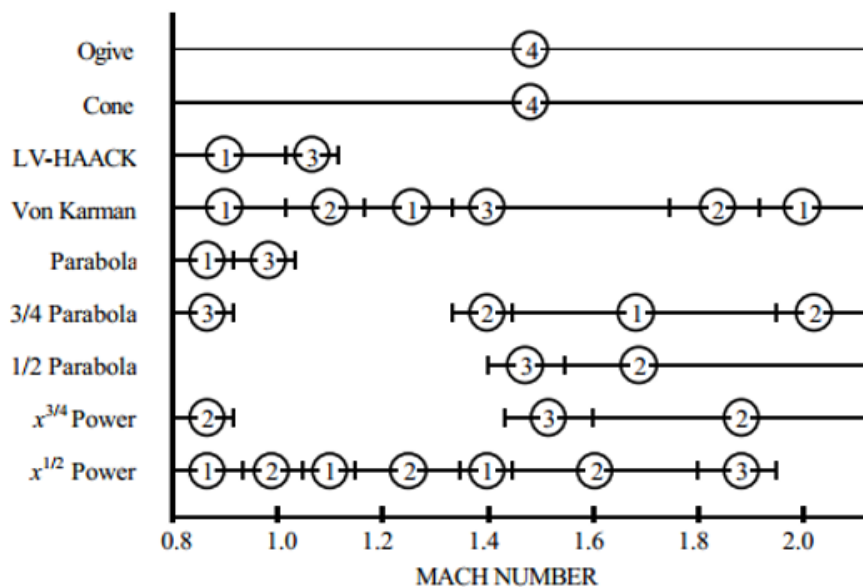


Figure 5: Nose cone profile as a function of mach number.[5]
1-ideal 2-good 3-acceptable 4-unacceptable

In order to create a profile that matches $x^{0.5}$, the surface of the cone must follow Equation (7). After the surface profile of the cone has been developed, the ideal length must be determined using the fineness ratio defined in Equation (8). The fineness ratio dictates the magnitude of wave drag experienced by the rocket as velocity increases. A high fineness ratio indicates a minimization in wave drag, however raising the fineness ratio requires making the rocket longer; a longer nose cone has increased surface area and thus a higher magnitude of surface drag is produced. As such optimization must be done to determine a specific nose cone length.

$$Y = \text{Radius of tube} * (x/\text{length of nose cone})^{0.5} \quad (7)$$

$$\text{Fineness} = \text{Length}/\text{Base Diameter} \quad (8)$$

6.5 Airframe Material Selection

Material selection for a rocket is crucial to its performance. Materials used for the body are required to withstand high speed ground impacts and undergo large changes in acceleration. As an added issue, the thrust to weight ratio is extremely important for a high power rocket; lighter rockets allow for the use of smaller motors and can potentially reduce overall cost. Meeting all of these conditions requires a high-performance material.

A computer program was developed to determine if a given material could meet the design requirements for safety and performance. The code analyzes the main tube of the vehicle as a hollow beam in compression. Data from the simulated flight of the vehicle, including the maximum thrust from the motor, the maximum drag force on the nose of the rocket, and the maximum force of the payload at maximum acceleration. These forces, with the latter two on top and the thrust force on the bottom, can be combined to determine the factors of safety for buckling of the beam based on expected load and the theoretical maximum compression the airframe may undergo before failure. Three materials were analyzed: Aluminum 6061, High Modulus Carbon Fibre, and Fiberglass.

Given a hollow, cylindrical airframe cross-section, a number of parameters related to buckling failure can be determined. The slenderness ratio of the airframe (beam) is given by

$$S_r = \frac{l}{k}, \quad (9)$$

where l is the estimated length of the vehicle [6] and k is the radius of gyration given by

$$k = \sqrt{\frac{I}{A}}. \quad (10)$$

In (10), I is the second moment of area and A is the cross-sectional area bearing the load. Using these parameters as well as the values for the compressive yield strength, S_{yc} , and compressive modulus, E , the critical loading of the airframe can be determined. The critical load is given by the Euler-column formula as

$$P_{cr} = \frac{\pi^2 EA}{S_r^2}. \quad (11)$$

A general stress curve based on the Euler equation is shown in Figure (6). When the slenderness ratio S_r is greater than a parameter given by

$$(S_r)_D = \pi \sqrt{\frac{2E}{S_{yc}}}, \quad (12)$$

which is determined from the intersection of the compressive yield stress and the stress

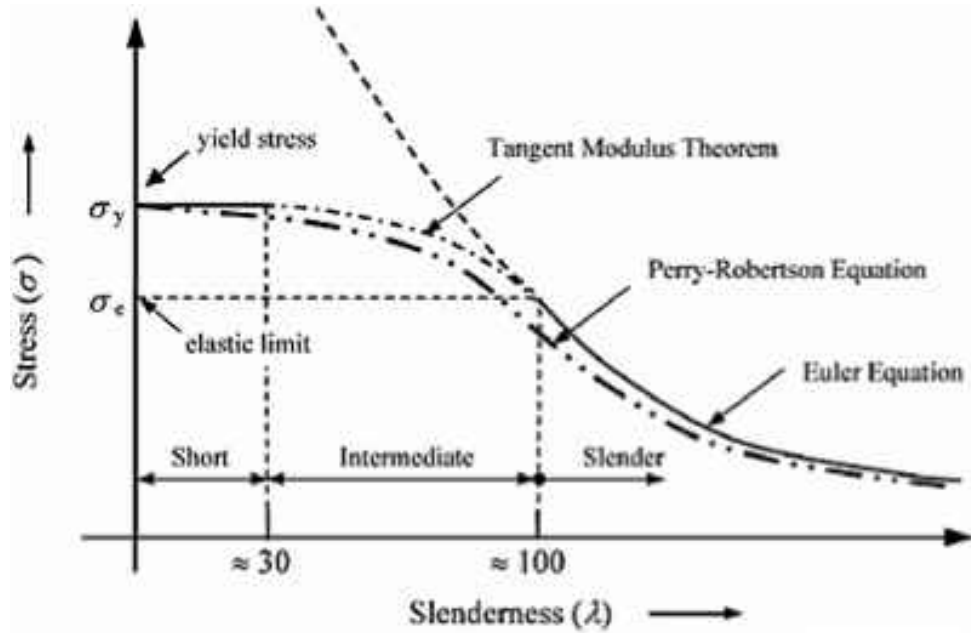


Figure 6: Stress vs slenderness ratio curve showing regions of safety known as Euler and Johnson regions.

curve, the Euler-column stress equation is used:

$$\sigma_{cr} = \frac{P_{cr}}{A} = \frac{\pi^2 E}{S_r^2}. \quad (13)$$

However if $S_r \leq (S_r)_D$ then the Johnson equation is used to determine the critical stress, given by

$$\sigma_{cr} = \frac{P_{cr}}{A} = S_{yc} - \frac{1}{E} \left(\frac{S_{yc} S_r}{2\pi} \right)^2. \quad (14)$$

Using these equations it is possible to determine the factors of safety for any material. This analysis can provide a good estimate of the necessary thickness for a particular material.

6.5.1 Aluminum 6061

Using aluminum to make the body of the tube yields a very high factor of safety as can be seen in Figure (46). The optimal point may be ignored in order to maximize the flight performance of the vehicle. To achieve the target apogee of 3048 meters, the buckling factor of safety will be greater than 100.

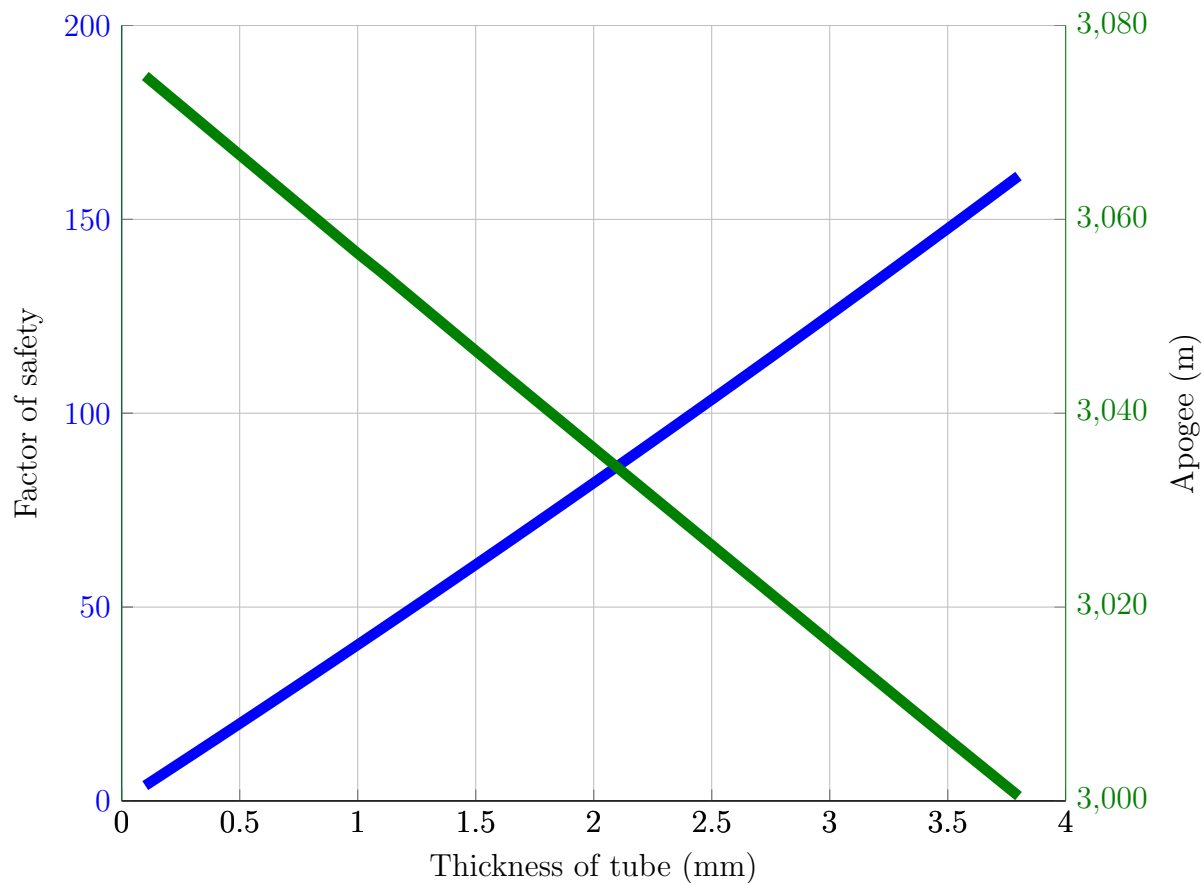


Figure 7: Plot of buckling factor of safety and apogee versus increasing tube thickness.

6.5.2 High Modulus Carbon Fibre

Since carbon fibre is weak in compression, the expected buckling factor of safety is quite low. To reach the target apogee, the factor of safety would be less than 10.

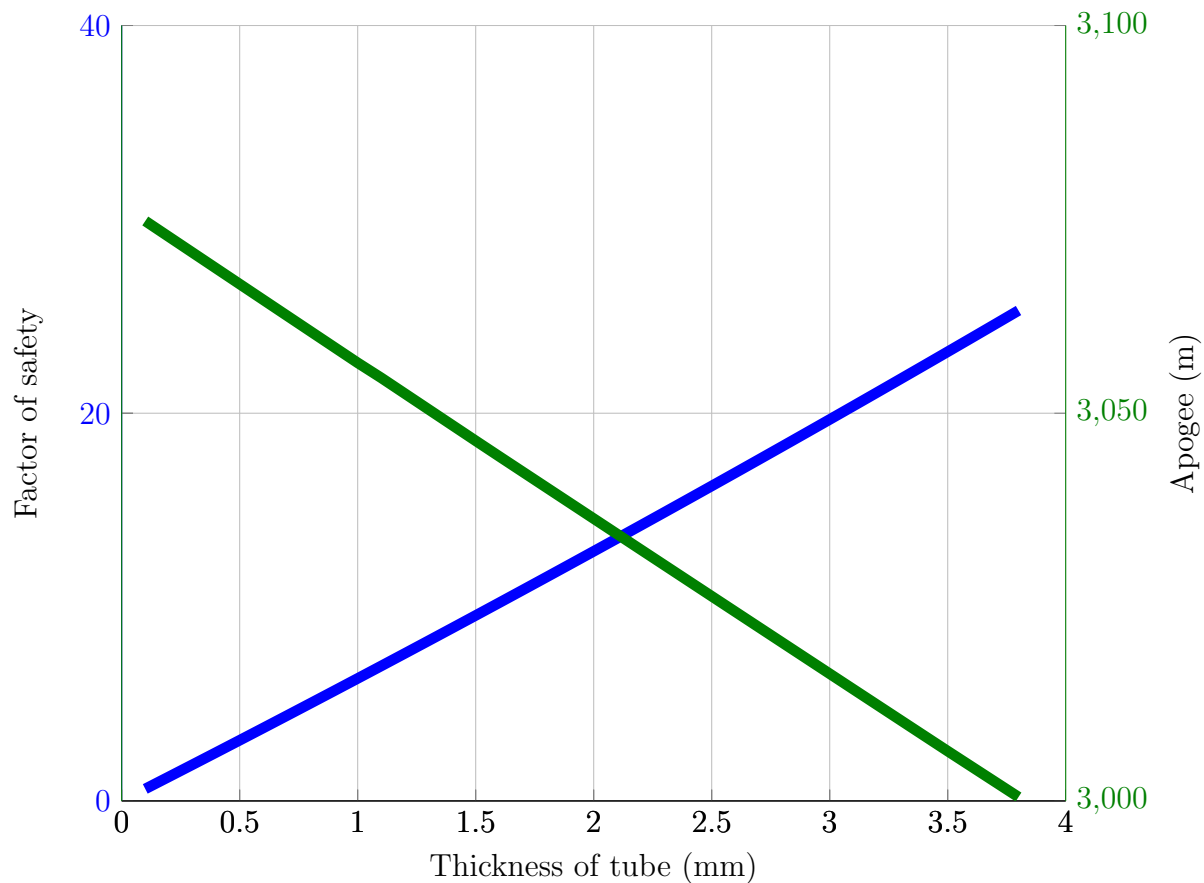


Figure 8: Plot of buckling factor of safety and apogee versus increasing tube thickness using carbon fibre.

6.5.3 Fiberglass

As can be seen in Figure (48), the expected buckling factor of safety while attaining the target altitude would be approximately 35. This is significantly higher than the factor of safety for carbon fibre.

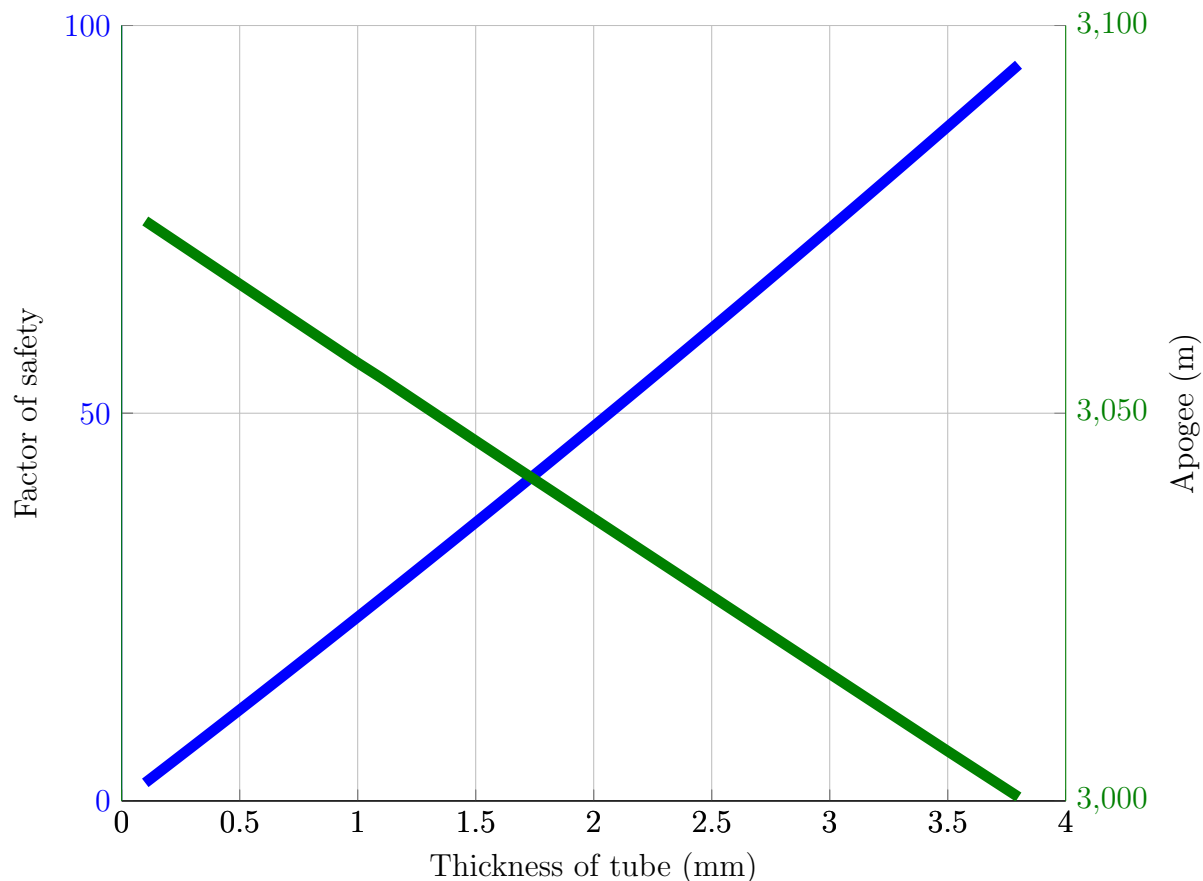


Figure 9: Plot of buckling factor of safety and apogee versus increasing tube thickness using fiberglass.

6.5.4 Selection

Given that the fiberglass gives the best buckling factor of safety for the lowest cost, the team has chosen it as the prime material to make the rocket out of.

6.6 Stability

Many different options exist for stabilizing the flight of a rocket. Of all possible options, it was deemed that fixed fins would be a cheap and effective solution to the problem. Since our rocket has an intended altitude of 10,000 ft AGL and a short flight time, the developmental cost and time required for any other stabilization systems would be unnecessary.

Although stabilizing fins work to align the rocket in a straight, steady flight, they also serve an additional function. In rocketry, the proximity between the center of gravity and the center of pressure is crucial to obtaining a stable flight; for desirable flight characteristics the center of pressure needs to be beneath the center of gravity by approximately 1

to 1.5 diameters of the rocket. Should the center of pressure lie any closer to the center of gravity, the fins are designed with increased surface area to move the center of pressure closer to the rear of the rocket.

6.7 Recovery Systems

The recovery system is very important for a sub-orbital rocket flying over land. In this competition the team has the dual purpose of ensuring that the vehicle comes down safely without harming anyone, and also protecting the valuable flight computer and payload sensors.

The recovery system of this rocket is split into two components: a drag device (parachute or parafoil), which slows the descent of the rocket, and the deployment system, which is responsible for ejecting the parachute from the rocket body reliably. The two components are separate entities which work in conjunction to bring the vehicle down safely.

6.7.1 Parachute System

There are three parachute systems that are currently the most often used in the amateur rocketry field: These are a dual deployment parachute system, a reefed parachute system, and a steerable parafoil system.

A dual deployment system includes a small drogue parachute which is ejected from the rocket at apogee. The drogue parachute slows the rocket initially and minimizes lateral drift from the launch site. When the rocket has reached a substantially lower altitude (1,500 ft AGL for the competition) the larger main parachute is deployed, and slows the rocket to an acceptable landing velocity. An example is illustrated in the figure below.



Figure 10: A dual deployment parachute system after deployment.
[7]

A reefed parachute system deploys a parachute at apogee, however the parachute is not fully developed until much later. It remains in a half-opened state for the majority of the descent. This allows the rocket to continue down at a high velocity, reducing drift substantially. Once the desired altitude has been reached, a ripcord is cut, which unreefs the parachute, allowing full expansion, and slows the rocket. An example is shown below.



Figure 11: A large-scale reefed parachute system after deployment, still in its reefed stage.
[9]

Steerable parafoils are much more complex. They work similarly to a dual deployment system, however instead of a main parachute, a parafoil is used. Small servos adjust the length of cables attached to the foil and steer the rocket down. However, in order for this system to work the rocket must have substantial mass. A steerable parafoil system is shown in the figure below.

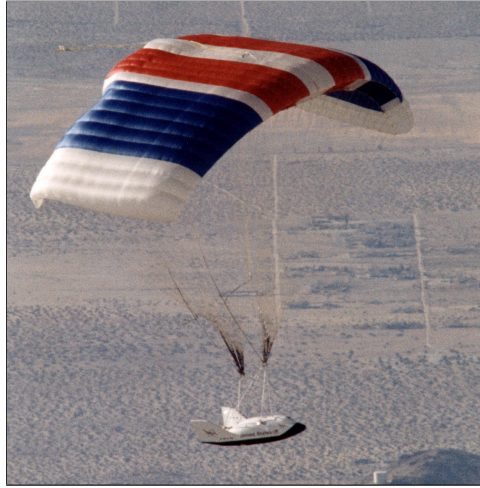


Figure 12: A steerable parafoil guiding an experimental flight vehicle.
[8]

In order to select a parachute system, a Pugh matrix was employed. Dual deployment is the most prevalent of the three systems in use and was chosen as the baseline.

Engineering Characteristics	Weight	Dual Deployment	Reefed Parachute	Steerable Parafoil
Mass	3	S	+	-
Reliability	3	S	-	-
Cost	2	S	S	-
Range Requirement	3	S	S	+
Complexity	1	S	+	-
Totals		0	1	-6

Figure 13: Pugh Selection Matrix for Recovery System showing that with the selected engineering characteristics, the reefed parachute narrowly scores more points than the baseline.

However, since there is an emphasis placed on safety and reliability for this competition, Team 24 has opted to use a conventional dual deployment parachute system. In addition, by comparing how each system performs according to the team's desired characteristics utilizing Figure (13), it was determined that a steerable parachute would be unreasonable and inefficient. Therefore, it was decided that there will be no attempt to incorporate a

steerable system into the dual deployment set up that Team 24 has chosen.

In order to determine the exact sizes needed for the parachute system, the calculation of the diameter of the parachute is based upon the desired ground impact velocity of the falling rocket. This was done using by using the equation

$$D = \sqrt{\frac{8mg}{\rho r C_d v^2}}, \quad (15)$$

where m is the mass of the rocket in kilograms, g is the force of gravity, ρ is the approximate density of air ($1.22kg/m^3$), C_d is the drag coefficient of the parachute, and v is the desired descent velocity.

By selecting a descent velocity of 12 fps it was determined that a 13 ft. diameter parachute would be needed for our main parachute. A B2 Rocketry XXL parachute was selected as it met our needs and budget.

Similarly by using a desired velocity value of 95 fps in (15) a diameter of 3 ft. is ideal for the drogue parachute. A Rocket-Man 3ft parachute was selected.

6.7.2 Deployment System

Multiple methods exist to eject a recovery system from the rocket body. The system must be reliable, not just on the ground but at the high altitude with lower atmospheric pressure that it will be deployed. There are two leading systems that could be chosen.

In the first design, a cartridge of compressed gas is punctured and the escaping gas is used to propel the parachute out of the vehicle. A commercial product is available and shown below for reference.

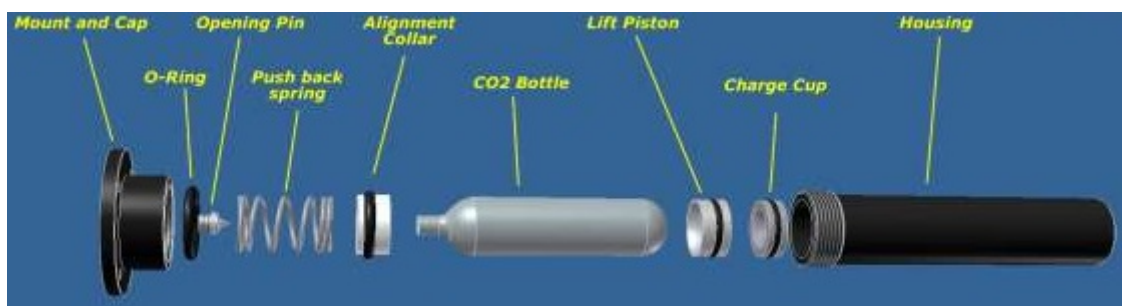


Figure 14: Exploded view of the Peregrine compressed CO₂ ejection system.

[10]

An alternative method is a black powder gas generator. This works by using a delay grain that holds a flame between the time of engine shutdown and apogee. Then the fuse

strikes a powder charge, producing a high temperature, high pressure gas that can eject the parachute out of the vehicle.

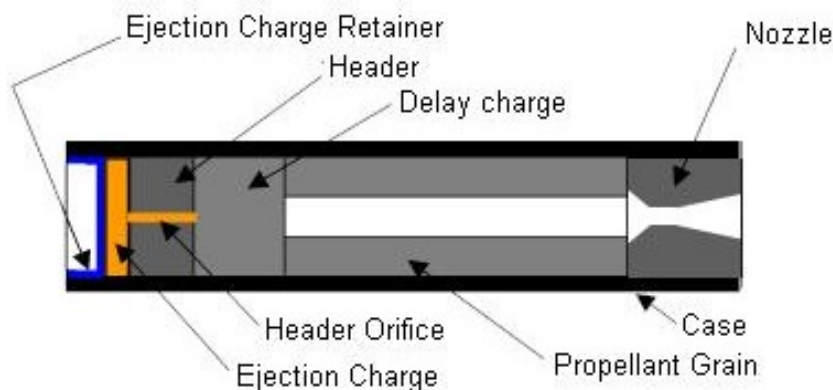


Figure 15: A simple diagram of a rocket motor with the gas generator on the left side at the forward end of the motor.

[11]

Black powder charges can also be ignited on demand via use of the flight computer. These systems eliminate the need for a delay grain and allow for precise timing of parachute deployment.

For the sake of minimal weight, the team has decided to use black powder gas generators ignited by our avionics system. This does however create additional design issues for Team 24. The avionics packages must now be protected from the hot gases created by the black powder. This is solved by creating a pill body section which will encapsulate the avionics and protect them. Further detail on this is available in the avionics section.

Combining all of the information gained, it was determined that the following layout would be ideal for the dual deployment system.

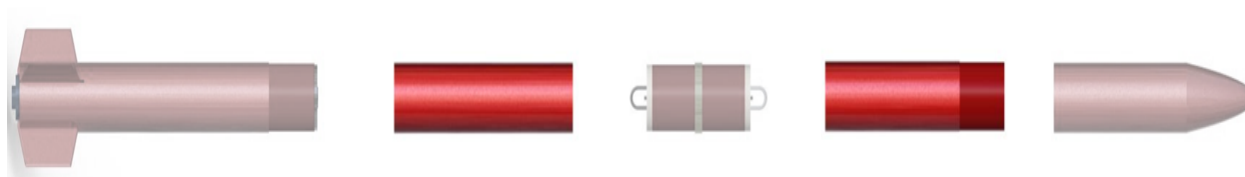


Figure 16: Rocketman 3ft Parachute and B2 XXL parachute contained in the main parachute and drogue parachute bays.

As can be seen in Figure (16) the drogue parachute will be located fore of the booster section. These two sections will be affixed in flight via metal pins and will not be allowed to separate from each other. This combined section will then be attached to the avionics bay by sheer pins which will be broken when the black powder charge ejects. An identical setup will be used for the main parachute bay and the nose cone.

6.8 Avionics

For the avionics package, the team has decided to purchase two commercial flight computers. Currently, commercial options are limited in their functionality, however they offer reliability which far exceeds what we would be capable of designing. The IREC rules show a clear preference towards safety and reliability and Team 24 has chosen to respect this by choosing the most reliable systems possible.

To meet this goal a StratoLoggerCF was selected as our main flight computer. The CF variant is a smaller version of the standard system and has the capability of igniting two flight charges at desired altitudes with a sensitivity of 100 feet. Additionally, the StratoLogger system records flight data including altitude, temperature, and battery voltage at a rate of 20Hz and records up to 18 flights on its chip. These flight recordings can then be downloaded to a windows desktop and Team 24 can analyze our flight characteristics.

The second flight computer is intended to serve as a backup system, if the primary altimeter becomes inoperable during flight or fails to deploy the parachutes at the appropriate times. We chose the RRC3 Sport altimeter to fill this role and satisfy the competition requirements for redundant electronics. Like the StratoLogger CF this altimeter is equipped with dual-deployment capability and is powered by a 9V battery. It records altitude and velocity at a rate of 20 Hz and, and both temperature and battery voltage at 1 Hz. The device also allows the user to download and plot the recorded data using a USB interface module and the MissileWorks mDACS PC software. Also, a total of 15 consecutive flights can be recorded on the RRC3 altimeter. In short, the RRC3 is comparable to the Stratologger CF and is and can perform the necessary deployment functions should the need arise.

6.9 Payload Design

The launch vehicle must carry an experimental payload. Through discussions with the team's mentor, a leading concept has been proposed. To leverage the ongoing research by the team's mentor and others at the Aero-Propulsion, Mechatronics and Energy (AME) Center, it is likely that the team's experiment will consist of an active flow control test-bed. This experiment will study the effects of injecting momentum in a fluid. Specifically, the intention is to separate the airflow downstream from the nose of the vehicle, and then inject fluid via injectors embedded in small ports around the circumference of the airframe in order to reattach the flow and modify the wake characteristics of the vehicle. This has the potential to improve drag characteristics for launch vehicles of this kind. The idea is also widely applicable in the field of aeronautics. Such experiments have been done before at the AME to modify the stall characteristics of aircraft, as seen in the

figure below.

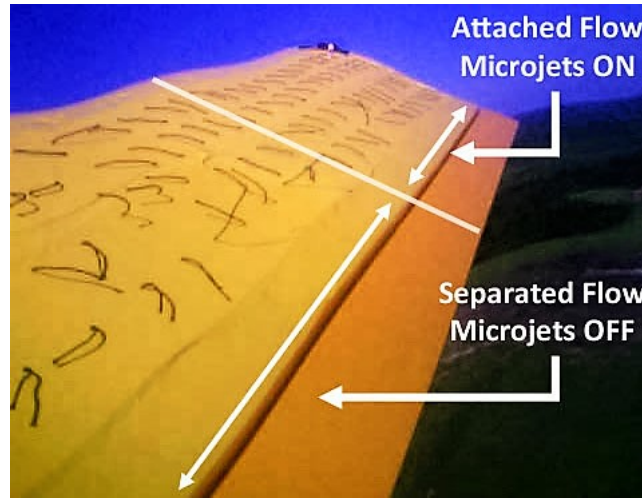


Figure 17: Flow injectors modify the stall characteristics of an experimental aircraft. [12]

To meet the requirements of the competition, the components of the payload designed must be able to fit in a standardized size. The competition uses the CubeSat, or U-class spacecraft, standard for the dimensions of the payload. These are denoted by

Size	Dimensions (cm ³)
1U	10 × 10 × 10
1.5U	10 × 10 × 15
2U	10 × 10 × 20
3U	10 × 10 × 30

Table 3: Standard CubeSat dimensions that the payload components must fit within.

For reference, a rendering is provided of the CubeSat frames in the figure below

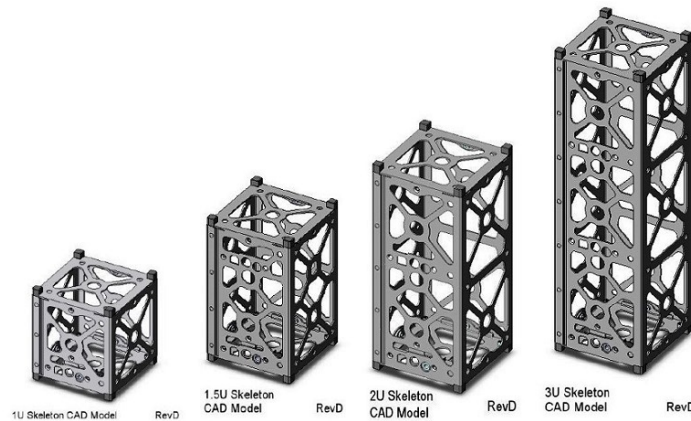


Figure 18: Comparison of standard cubesat frames. [13]

7. Final Vehicle Specifications

In order to determine the exact physical characteristics of the rocket, Team 24 has taken an iterative approach based upon component selection and weight information. After each successive design, the weight and size information from the model was added into the calculations and used to refine the design requirements. After several iterations, Team 24 developed the rocket shown in Figure (19) and Figure (20).



Figure 19: View 1 of the final launch vehicle.



Figure 20: View 2 of the final launch vehicle.

7.1 Launch Vehicle Overview

To recap to previous information, the pertinent design decisions have been tabulated below.

Subsystem Selection	
Nose Cone	$x^{1/2}$ Profile
Airframe Material	Fiberglass
Stabilization	Fixed Fins
Recovery System	Dual Deployment
Deployment System	Black Powder Gas Generator
Flight Computer	Commercial System
Experimental Payload	Active Flow Control Testbed

Table 4: Overview of launch vehicle subsystem decisions.

To house all of these components the team has decided to use a 5 section design with integrated section couplers. By using a modular section design Team 24 has provided for the ability to quickly change sections and components independently of other sections and components as well as allow for rapid assembly and dis-assembly. Furthermore, this construction method serves a second purpose of providing an easy parachute deployment method which does not require any additional bays or doors.

The 5 main sections are shown in Figure (21).

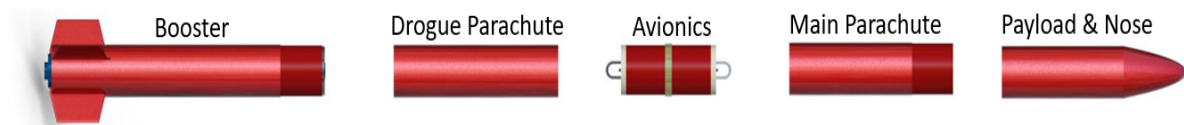


Figure 21: The 5 main rocket sections in order of assembly.

Each of these sections are housed within 2mm thick fiberglass tubes with an inner diameter of 152mm. This diameter was determined by the requirements of the CubeSat unit which has a diagonal of 141mm. As such this meant that our minimum diameter for that section had to provide enough clearance for the mounting solution we have designed. For simplicity of construction, and reduction in calculation complexity, it was determined that all sections will conform to the same diameter.

7.2 Booster

The booster section of the rocket houses the propulsion system and thrust structure. The thrust structure is necessary to ensure that the load from the motor can be adequately distributed through the body of the rocket without damaging anything. It also serves the purpose of attaching the stabilization fins. The booster is shown in detail in Figure (22). The chosen motor is the Cesaroni Technology Incorporated M1450P solid rocket motor.

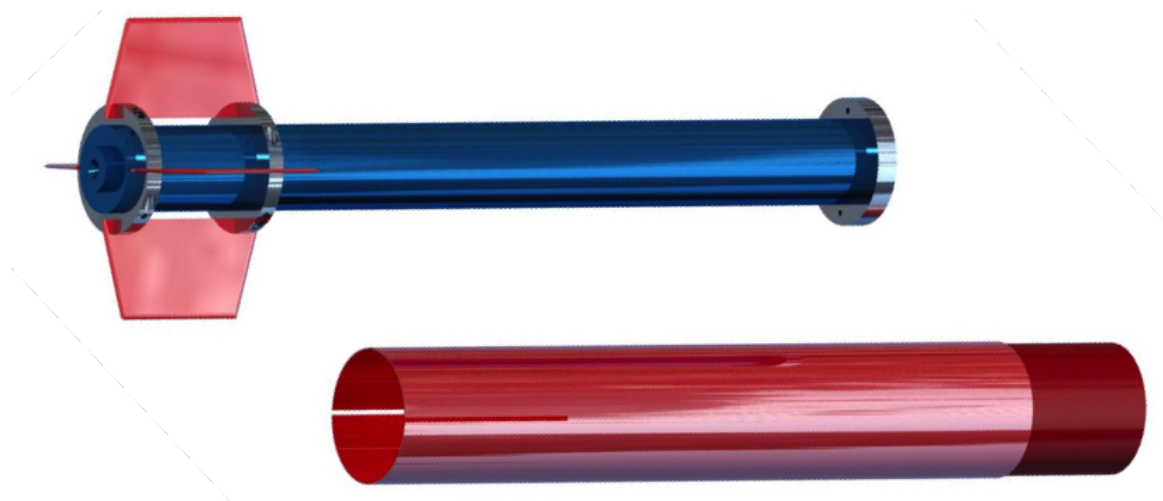


Figure 22: Detailed view of the rocket motor casing, thrust structure, stabilization fins, and housing tube.

The booster relies on centering rings to hold the rocket motor in the center of the booster tube. These centering rings primarily serve the purpose of distributing the loading from the thrust of the motor during the burn. They are made of machined aluminum and are connected to the fiberglass tube using a number of M8x1.25 stainless steel machine screws. The main centering ring, between the top and bottom centering ring is shown in Figure (23) below. The holes drilled into the side of the centering perpendicular to the fin slots are used to hold the fins in place.



Figure 23: Detailed view of the main centering ring.

7.3 Drogue Parachute Section

Immediately following the Booster section will be the Drogue Parachute bay shown in Figure (24).



Figure 24: The drogue bay shown immediately following the booster section. In this section the parachute is represented by a brown cylinder and the kevlar shock cord is not shown to increase view-ability.

This section will be 24 inches long and have a 6 inch section on each side which will overlap the adjacent sections. Housed within the fiberglass body tube will 15 feet of 1 inch diameter kevlar shock chord which will be mounted to a drop forged shoulder eye bolt on both of the contiguous sections. Bisecting the shock cord will be the 3ft Rocket-Man parachute previously selected in section 6.7.1. The body tube will be affixed to the booster section during flight via 4 metal pins which are sufficiently strong enough to withstand the force created by the black powder charges. On the other end, the section will be attached to the avionics bay with #2 nylon shear pins. Shear pins are strong enough to maintain a rigid contact between the two sections, but will not be strong enough to hold the rocket together after the black powder charges in the avionics bay have been detonated.

7.4 Avionics Bay

The Avionics bay is the middle section of the rocket and is shown in Figure (25). For this section of the rocket it was determined that a medicinal pill inspired design would be ideal for housing and protecting the sensitive avionics components.

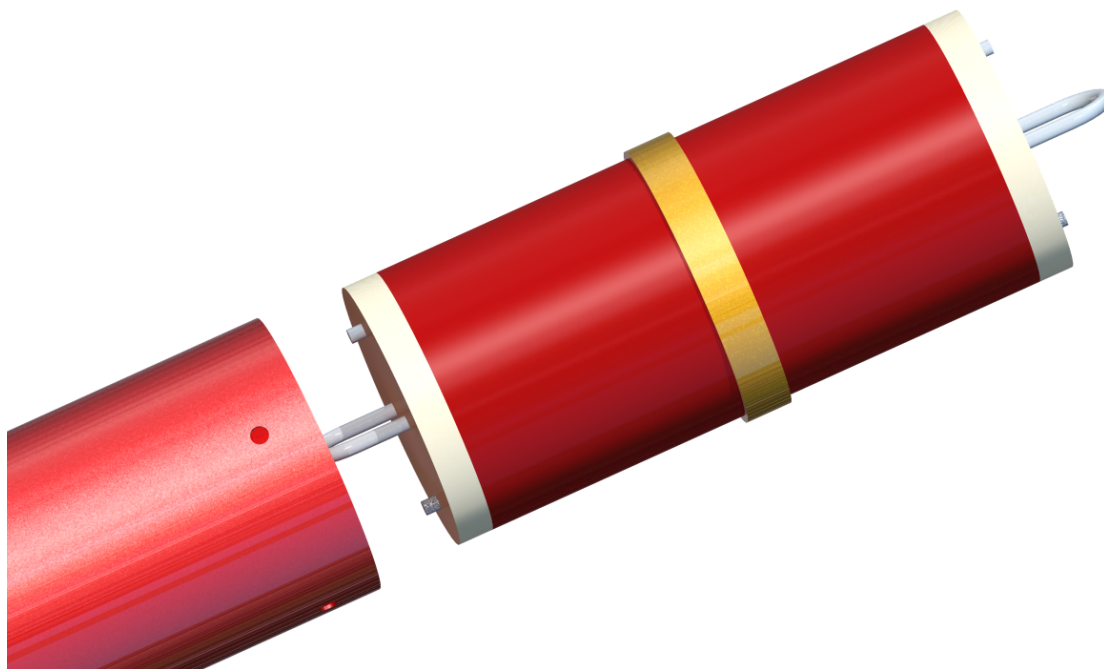


Figure 25: The avionics bay enclosed.

The total bay is 14 inches long with a 2 inch center band. The 6 inches on each side slide within the two parachute bays. This allows for a minimal addition in overall rocket length and serves as mounting locations for the kevlar shock cords and parachutes. An open view of the avionics bay is shown in Figure (26). Here it can be seen that all of the flight computer hardware is mounted on a sled held firmly in place via two $3/8$ inch threaded rods. These rods also serve to hold the entire assembly together by bolts on either side of the bottom and top avionics plates.

In order to adequately protect the electronics, it was determined that separation from the black powder charges would be necessary. This is addressed via two concentric $3/4$ inch plywood plates attached together as an end plug plate. Identical plates are mounted on either side of the avionics bay. Two small circular protrusions on each plate house the black powder charges. After being filled, these sections will be covered with masking tape to prevent the powder from falling out. Ignition will be handled via electric ignition from the selected avionics package from section (6.8).

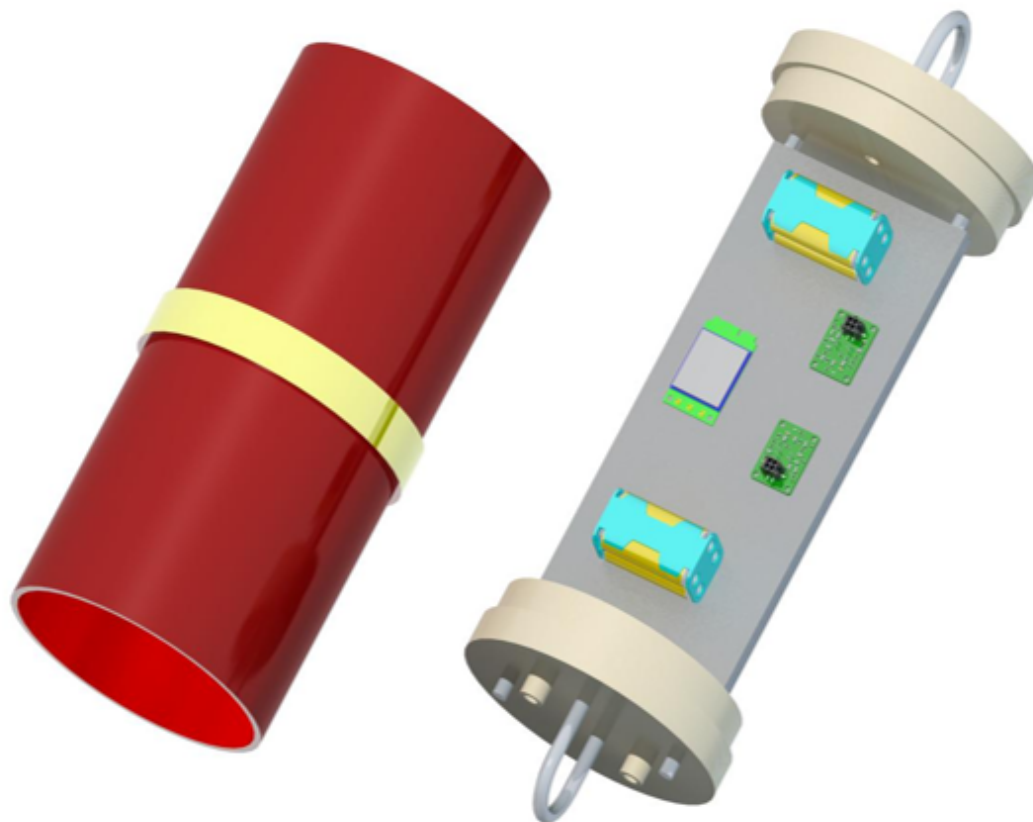


Figure 26: The avionics bay opened.

Represented by a grey sled in Figure (26), the avionics sled will serve as the mounting point for all of the electronic sensors and flight computers. This plate will be 3D printed from ABS plastic by the group. This will allow us to incorporate built in specific mounting locations for our exact flight computers requirements. Additionally it'll also have incorporated hocks for wire management.

Also mounted to this board will be a TELEGPS Radar beacon; the TELEGPS unit has been selected for locating our rocket after recovery. This works by emitting a signal which can be tracked with a hand-held unit.

Main and backup power will be supplied by Tenenergy Centura Nickel Metal Hydride batteries. This will allow for an independent power source for each of our flight computers. The battery containment modules will also be mounted onto the avionics bay.

All wiring for this bay will be handled with #24 Gauge Copper wiring. Capable of 2.5 amp power transferal, this gauge wiring is a standard for flight electronics and is a requirement for the IREC.

7.5 Main Parachute Section

Immediately following the Avionics Bay will be the Main Parachute section shown in Figure (27).

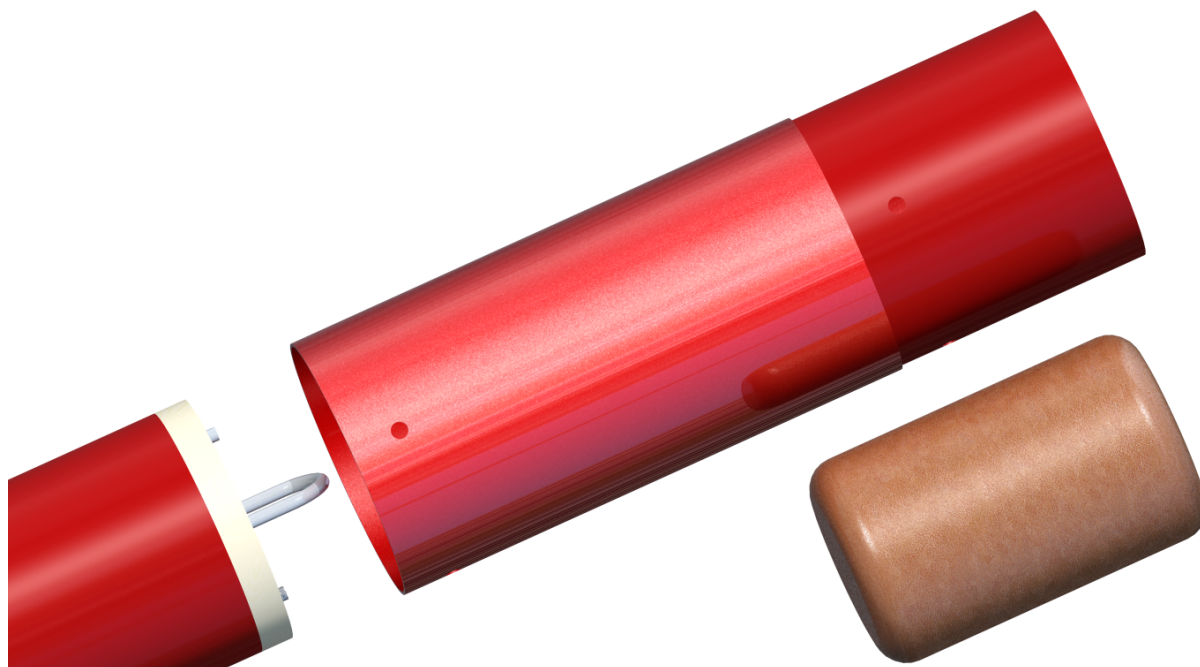


Figure 27: The main parachute bay shown immediately following the avionics bay. In this section the parachute is represented by a brown cylinder and the kevlar shock cord is not shown to increase view-ability.

This section will be 18 inches in overall length, but will have an attached coupler section which comprises one third of the total length. Since the first 6 inches will overlap onto the avionics bay, the main parachute and shock chord will be held inside of coupler portion of this section. 30ft of kevlar shock cord will be used for this section and will be attached to the avionics bay and the nose cone section. Bisecting this will be a B2 XXL parachute.

Attachment of this section to the adjacent sections will be done via #2 nylon shear pins and metal pins for the avionics and nose section respectively.

7.6 Nose Cone and Payload Bay

The payload will be housed inside of the nosecone section shown in Figure (28).



Figure 28: The payload will be housed inside of the nose cone and attached tube section.

There are two main body components to this section: the 18 inch fiberglass tube and the 11 inch nose cone. These sections are held together by epoxy and will be inseparable. The nose cone section shall be 3D printed from ABS plastic. Incorporated into the base of the nose cone is a square section which will serve as a mounting point for the CubeSat payload unit. This can be seen in Figure (39).

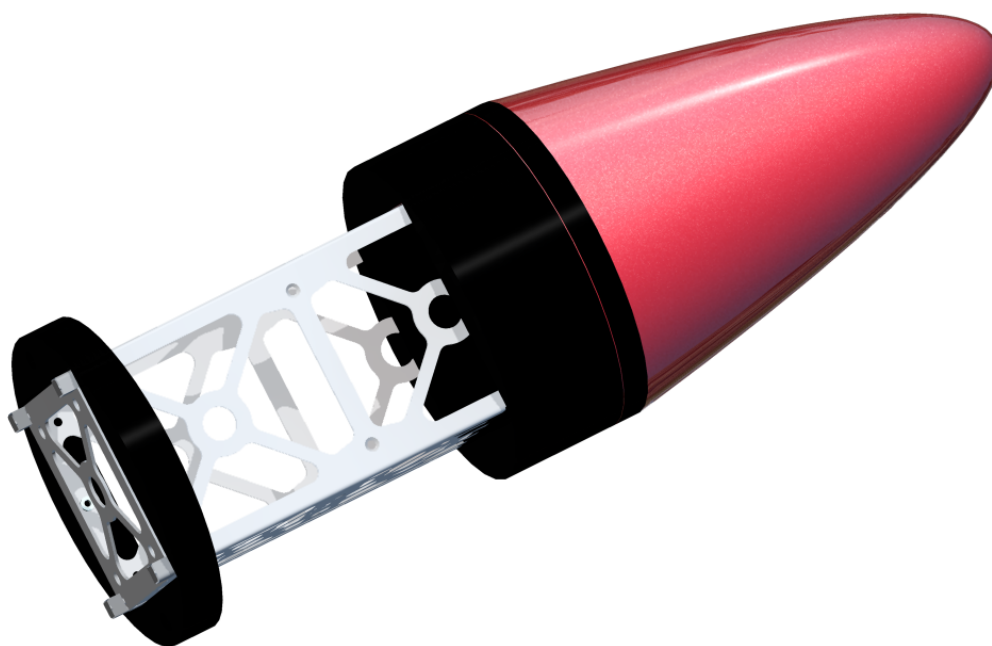


Figure 29: The nose cone with the payload section and centering ring.

An additional centering will be also be 3D printed from ABS plastic for anchoring the CubeSat payload to the fiberglass tube. Not shown in the Figures are the front-most rail button and the parachute mounting point. These shall be located inside of the fiberglass tube.

7.7 Cost Analysis

The total cost of the air-frame and interior components, not including tax, is shown below in Table (5). The total for all 5 sections comes to \$2,732.32.

Section	Cost
Booster	\$1570.00
Drogue Parachute	\$117.78
Avionics Bay	\$636.57
Main Parachute	\$331.9969
Nose Cone	\$75.98
Total	\$2732.32

Table 5: Cost breakdown of rocket into the 5 main sections.

Rocket fuel and the motor comprise the dominant cost of this rocket. The complete motor assembly costs \$1,389.89 before tax on the current market. This means that the cost of the rest of the rocket is only \$1,342.43 pre-tax. Therefore it is possible the entire airframe can be constructed sans-motor with our current budget of \$2000. Currently, Team 24 is looking into other funding for the extra funds required to purchase the motor and go to competition.

A complete cost breakdown of all components is available in the Appendix.

8. Launch Vehicle Validation

In order to verify that the final rocket design is capable of reaching 10,000ft AGL and is safely recoverable, Team 24 has utilized an additional simulation as well as performed a hardware failure analysis for our launch vehicle.

8.1 Structural Integrity Analysis

Analyzing the solid mechanics of a rocket can be useful to determine the required structural integrity of the rocket body. This analysis is vital when designing a high powered

rocket to ensure a safe launch and recovery. The finite element method was used to determine the von Mises stresses acting on the rocket. First, the rocket body was modeled as a simple tube where the motor's thrust was applied to one end and the other end held stationary. Next, the geometry of the rocket motor housing was added to the model. The motor's thrust was applied to the motor casing, and the opposite end of the rocket was held stationary. The von Mises stress acting on the rocket was determined to be approximately 950 kPa along the main body of the rocket, and stress concentrations at the junction between the rocket motor casing and rocket body were determined to be about 2.4 MPa.

8.1.1 Solid Mechanics

8.1.1.1 Assumptions

The rocket's motor is a CTI 9955M1450 solid propellant motor. The maximum thrust that this motor produces is about 2400 N. This can be seen below in Figure 30, which is a graph of the motor's thrust curve [14].

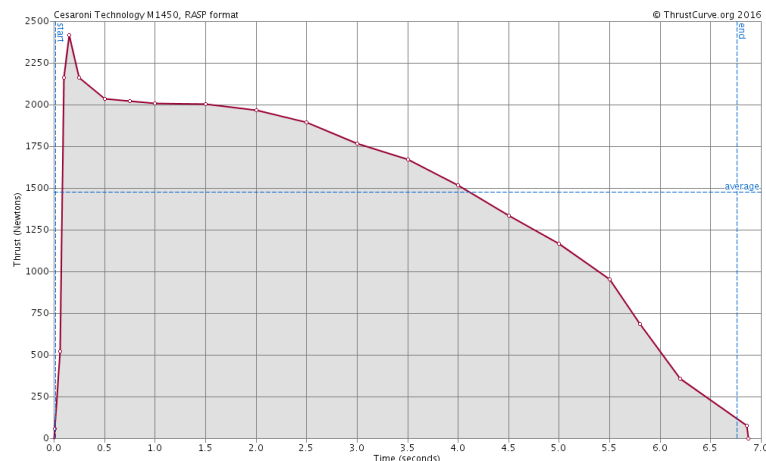


Figure 30: Thrust curve of the CTI 9955M1450 high power rocket motor [14]

The rocket's maximum velocity is predicted to be 540 mph, and this results in a drag force of 164 N. The maximum force of drag is 14x less than that of thrust. Additionally, the rocket's max thrust occurs 0.25 seconds into flight. At this time, the rocket has not yet reached its max velocity. Therefore, the force of drag will be neglected in the COMSOL model, and the load due to the motor's maximum thrust will be modeled and analyzed.

During the initial portion of the rocket's flight, it is undergoing about 6 G's of acceleration. In order to model the solid mechanics of the rocket, boundary conditions must be applied to make the rocket stationary. To keep the rocket stationary, the nose portion of the

rocket was assumed to be fixed. The acceleration's effect on the rocket body was also ignored.

Assumptions about the construction of the rocket were also made. The motor casing will be attached to the rocket's body via three centering rings. The points of attachment for the three centering rings were modeled as rigid attachments between the entire outer surface of the centering rings and the inner surface of the rocket body. In reality the centering rings will be attached to the rocket body using screws/pins, and the rocket body reinforced around each hole. The centering rings will also be attached to one another via long threaded rods. These rods were completely ignored, and this would result in the COMSOL model being less reinforced when compared to the actual rocket being modeled.

The rocket body was modeled as fiberglass, and the motor housing and centering rings were modeled from aluminum. COMSOL's built in material properties were used to define each material. The material properties of each can be seen below in Table 6 [16].

Material Property	Fiberglass	Aluminum
Young's Modulus (GPa)	85	70
Density kg/m^3	2600	2700
Poisson's Ratio	0.23	0.33

Table 6: Material Properties Used [16]

8.1.1.2 COMSOL Models of Simple Rocket Tube

The first COMSOL model used was extremely simple. It is a model of the upper portion of the rocket body not including the motor and also not including the nose cone. The model was first analyzed in 2D. Then it was revolved around a central axis and analyzed in 3D. The thrust from the motor, 2400 N, was applied to the lower portion of the rocket body. The upper edge of the rocket was constrained using a fixed boundary condition. This boundary condition was necessary for the COMSOL model, but it does not accurately reflect the constraints of the rocket during flight. Therefore, the stress concentrations near the top of the rocket due to the boundary constraints can be ignored. The resulting model shows an average von Mises stress of 970 kPa along the length of the 2D and 3D simplified COMSOL model. The simple 2D and simple 3D model can be seen below in Figure (31) and Figure (32) respectively.

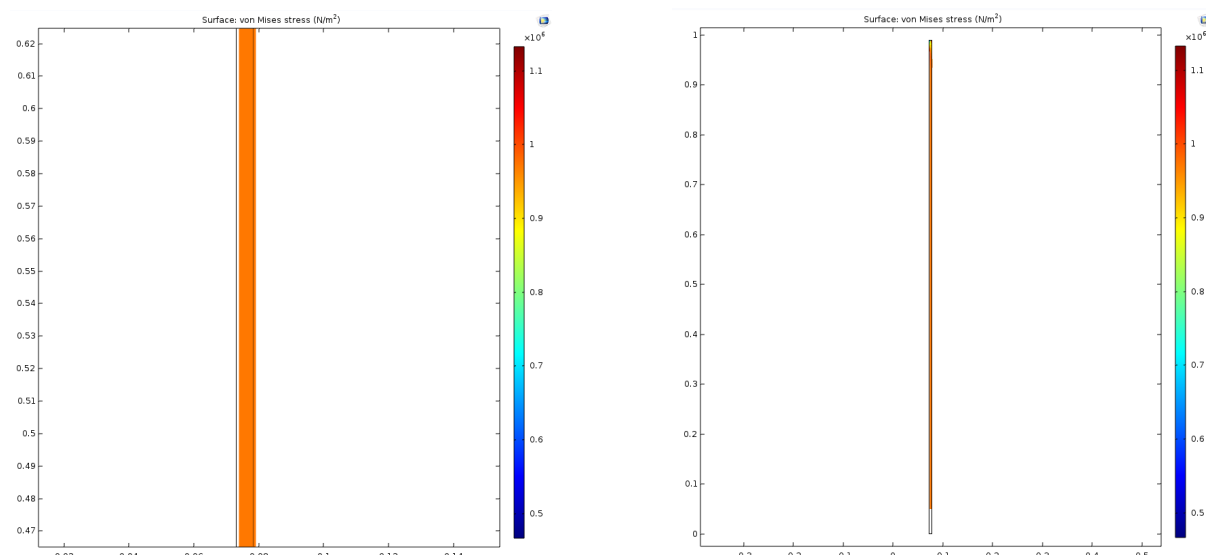


Figure 31: 2D COMSOL models of a simple rocket tube

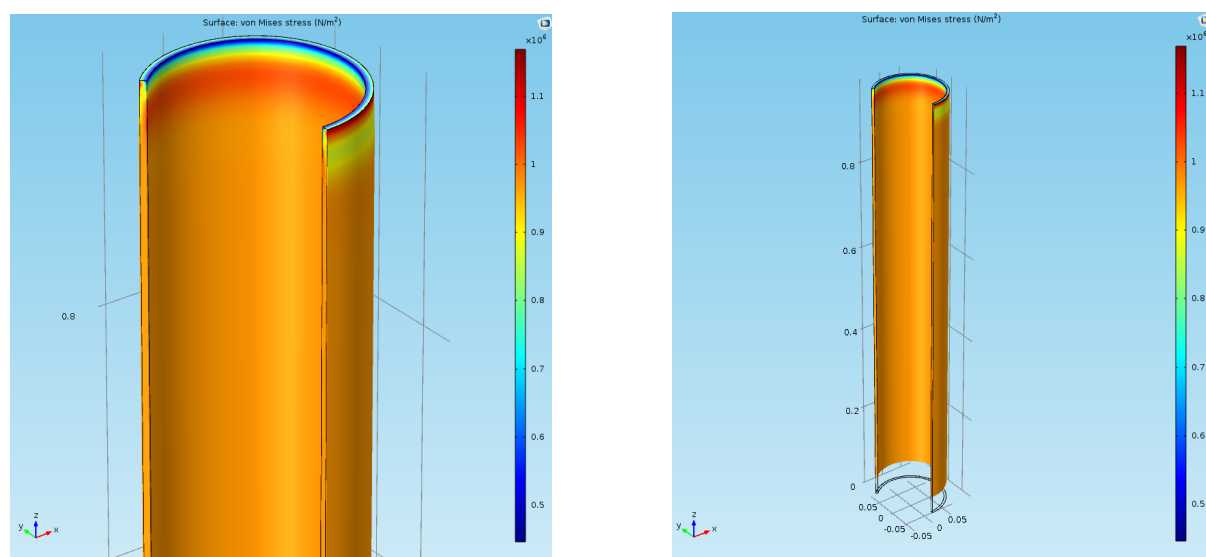


Figure 32: 3D COMSOL models of a simple rocket tube

8.1.1.3 COMSOL Models of Rocket Tube and Motor Housing

Next a more complex model of the rocket was made in 2D and then revolved to form a 3D cylinder. In this model, the rocket motor housing and centering rings were added, and the 2400 N load from the motor was applied the inner upper surface of the aluminum motor housing. The von Mises stress of the rocket tube was about 930 kPa in the 2D and 3D model, which is consistent with the simple model. There highest stress concentrations where the motor housing connects to the rocket body, and stress concentrations could also be seen at the center of motor housing, where the motor's thrust is directly applied. The maximum von Mises stress at the connection of the motor housing and body is about

2.7 MPa in 2D and 3.3 MPa in 3D, and the maximum von Mises stress on the motor housing was about 2.3 MPa in 2D and 2.4 MPa in 3D. The 2D and 3D model can be seen below in Figures (33) and (34).

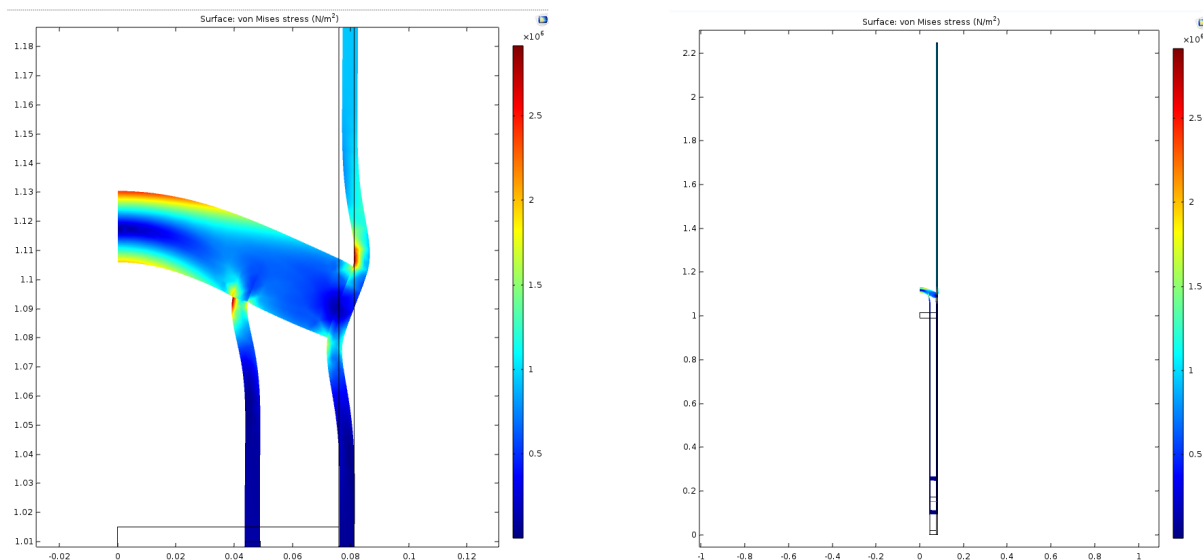


Figure 33: 2D COMSOL models of rocket tube and housing

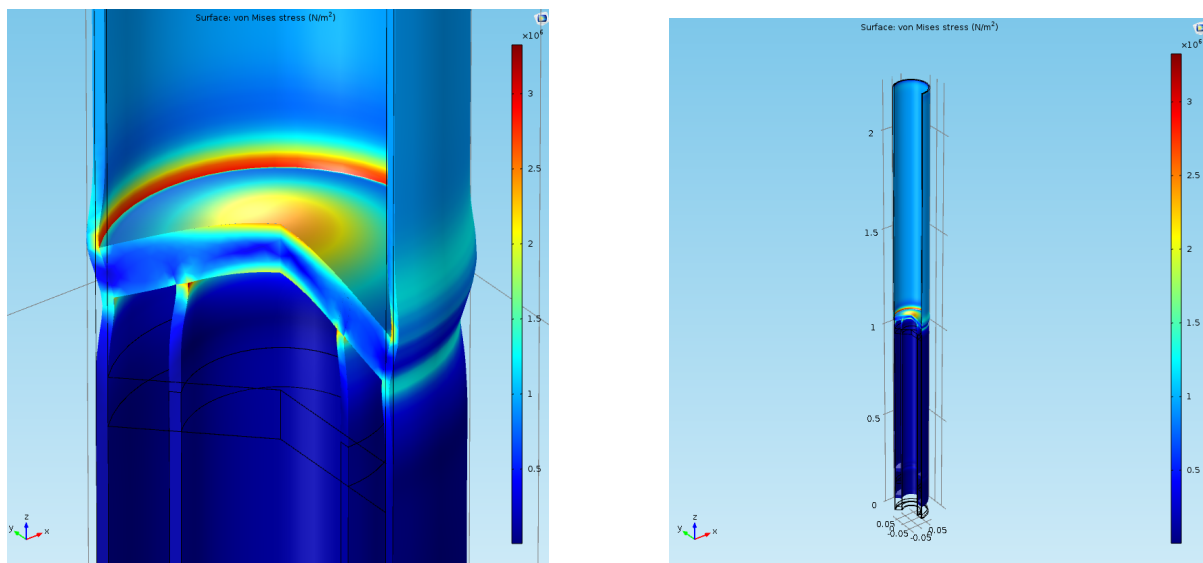


Figure 34: 3D COMSOL models of rocket tube and housing

8.1.1.4 Verification and Validation

In order to verify the model, hand calculations were made. The rocket was modeled as a thin walled tube under axial loading. The force applied was 2400 N and the cross sectional area was determined to be $2.519 \times 10^{-3} \text{m}^2$. From Equation (16) seen below, the

stress in the rocket body is 950 kPa.

$$\sigma = \frac{F}{A} \quad (16)$$

The simple COMSOL model had a von Mises stress of 970 kPa, and the COMSOL model including the motor housing had a von Mises stress of 930 kPa along the rocket body. This is reasonably close to the hand calculated value of 950 kPa.

The yield stress of aluminum is 90-290 MPa, so the calculated maximum of 2.5 MPa von Mises stress on the motor casing is not likely to cause a failure [15]. A failure in the motor casing is not expected because the motor casing is a commercial off the shelf product designed specifically designed for housing high powered rocketry motors.

8.2 Flight Performance Simulation

Before committing to any finalized designs and eventual purchases, it was necessary to assess the soundness of our design through analysis of rocket's flight performance in flight simulation.

Analysis of the rocket's flight performance was done using two methods. The first is using the previously mentioned program which was developed in-house, mostly using first principles. The second is an open-source software used by experimental rocketry designers called OpenRocket.

8.2.1 In-House Simulation

The details of the in-house simulation are explained in section 6.2. Using the fixed mass of our vehicle, the simulation is run to predict the apogee and mach regime encountered. These graphs are shown in Figures (50) and (51).

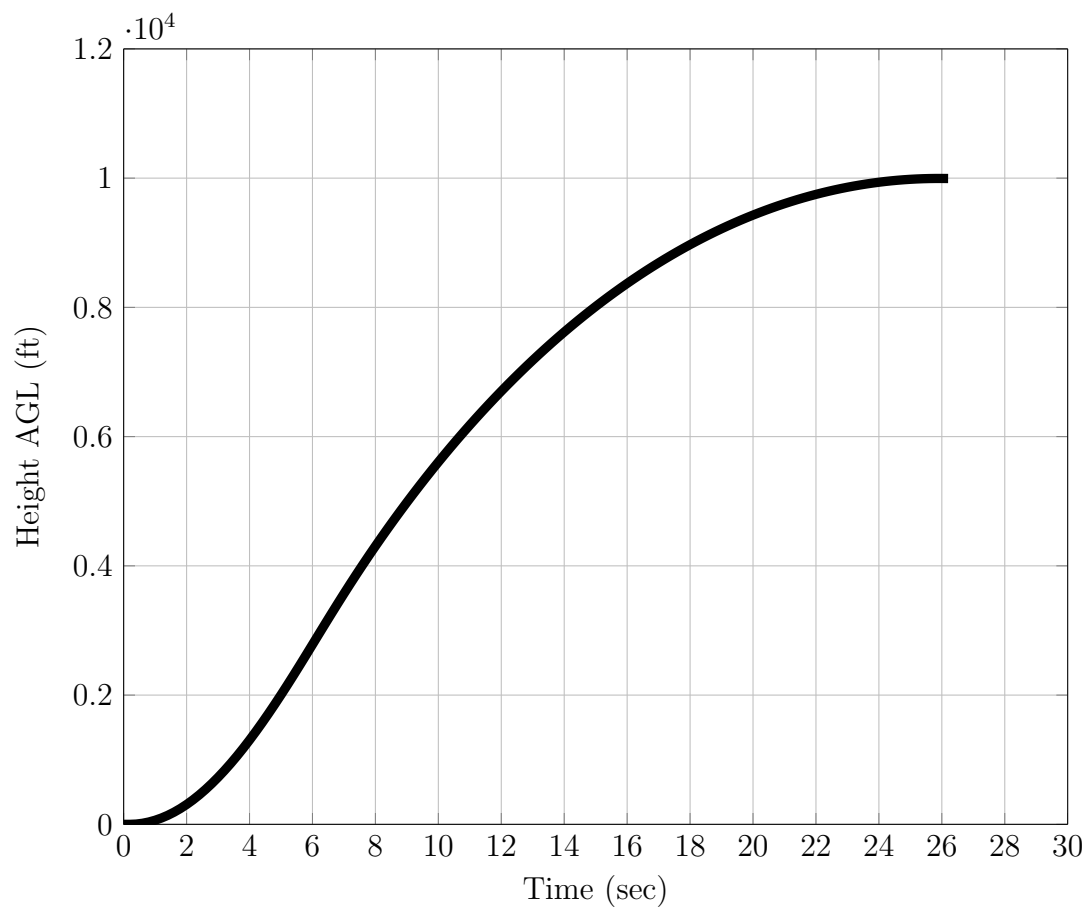


Figure 35: Plot of the height of the rocket AGL during the ascent phase of the flight.

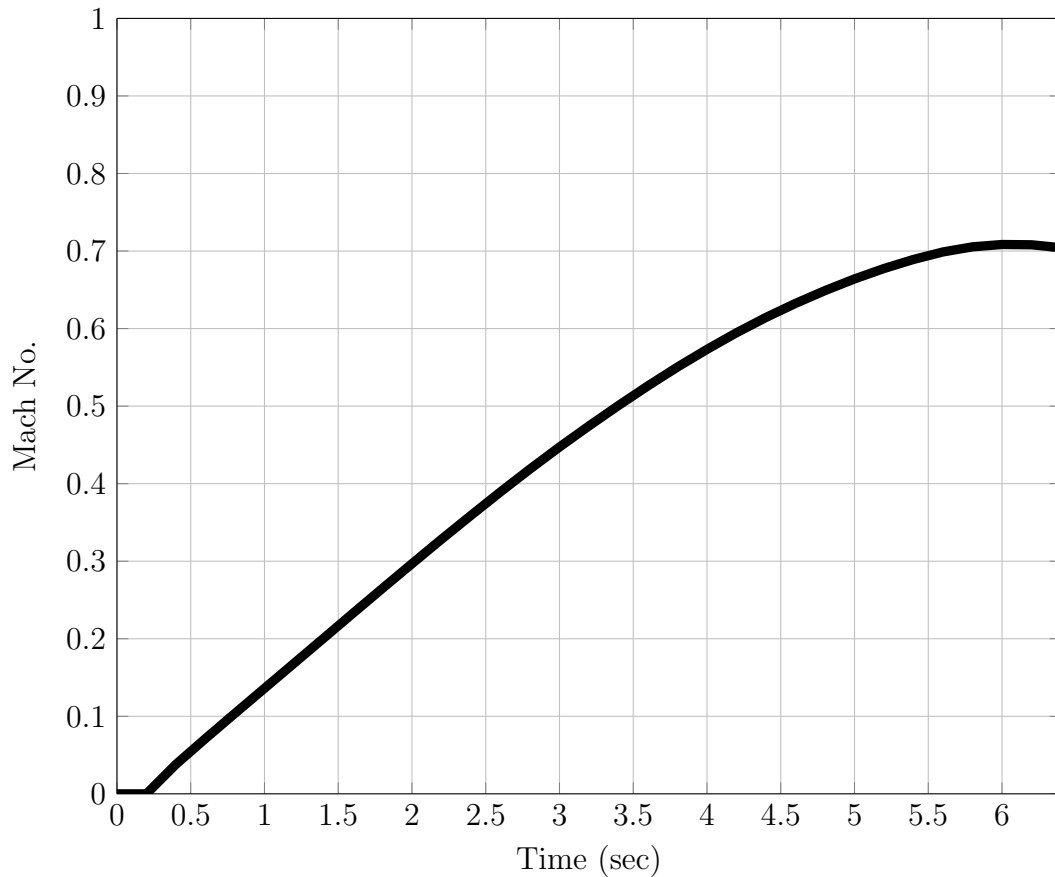


Figure 36: Plot of the mach number of the rocket during the motor burn.

8.2.2 OpenRocket

OpenRocket is one of the most commonly used means of rocket flight simulation among amateur rocketeers. Given its features, the software allowed Team 24 to make significant design choices affecting both stability and motor selection.

The simulation software allowed Team 24 to input the entirety of the rocket design, including each internal component in their respective locations. For example, the main parachute was defined in OpenRocket using its exact weight, dimensions, and location. The parachutes could also be set to deploy at specific times during the descent. The above image shows some of the rockets' components as they appear in the OpenRocket simulator. The software includes a database of materials and common brands for various components, meaning that the properties of the tube sections, the centering rings, parachutes, and so on were factored into each simulation.

The immediate benefit of OpenRocket was that even before the first simulation, we could see whether our rocket was both stable and powerful enough to reach the target apogee of 10,000 ft. Early simulations showed that the center of pressure was not in the necessary

location for the rocket to remain upright during the beginning of the flight. To remedy this, the fins were redesigned in OpenRocket, resulting in the center of pressure being placed about 7 in behind the center of gravity, where it would be more conducive to a stable flight.

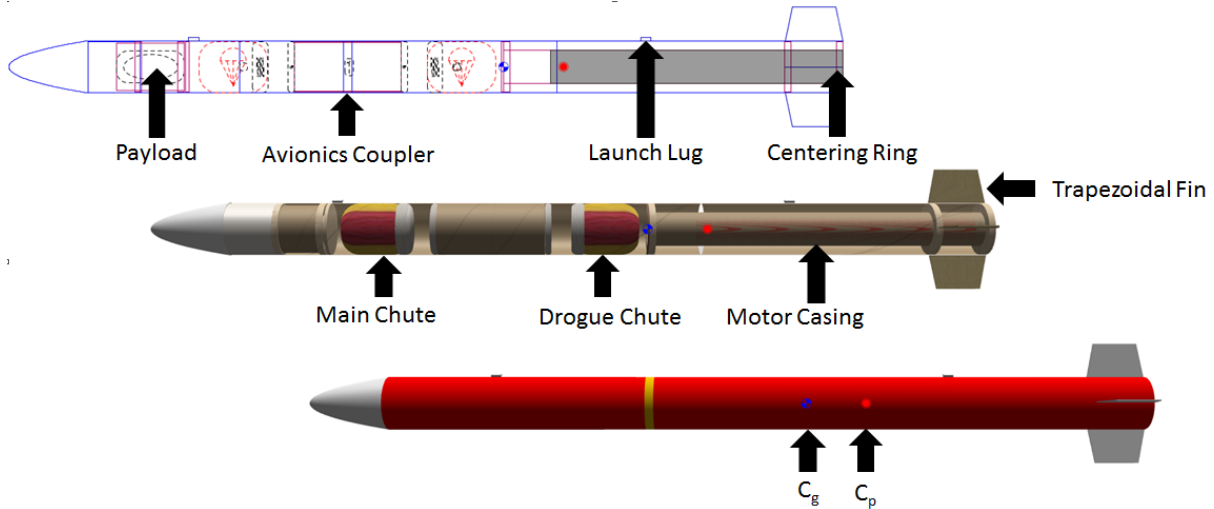


Figure 37: 2D and 3D graphics of the rocket design in OpenRocket.

Each simulation generated the altitude, velocity, and acceleration data based on the thrust curve, dimensions, and weight of the chosen motor. Using the motor that seemed the most promising during the conceptual design phase, the rocket fell short of target apogee by over 1,000 ft. After several iterations a more powerful motor was chosen, the Cesaroni M1450P, which could achieve an apogee above 10,000 ft and a maximum velocity equal to about 70% the speed of sound. These findings are reflected in the Table (7) below, which also compares data from the in-house simulation.

Property	In-House Simulation	OpenRocket
Apogee (<i>ft</i>)	10073	10082
Max. Velocity (<i>ft/s</i>)	799	794
Max. Acceleration (<i>ft/s²</i>)	214	214
Center of Gravity (<i>in</i>)	—	57.5
Center of Pressure (<i>in</i>)	—	65

Table 7: Comparison of data from the in-house simulation and OpenRocket.

In OpenRocket, we found that several different variables were tracked during each simulation. Beyond altitude, velocity, and acceleration, these included the drag force, angle of attack, propellant mass, and the location of the center of gravity.

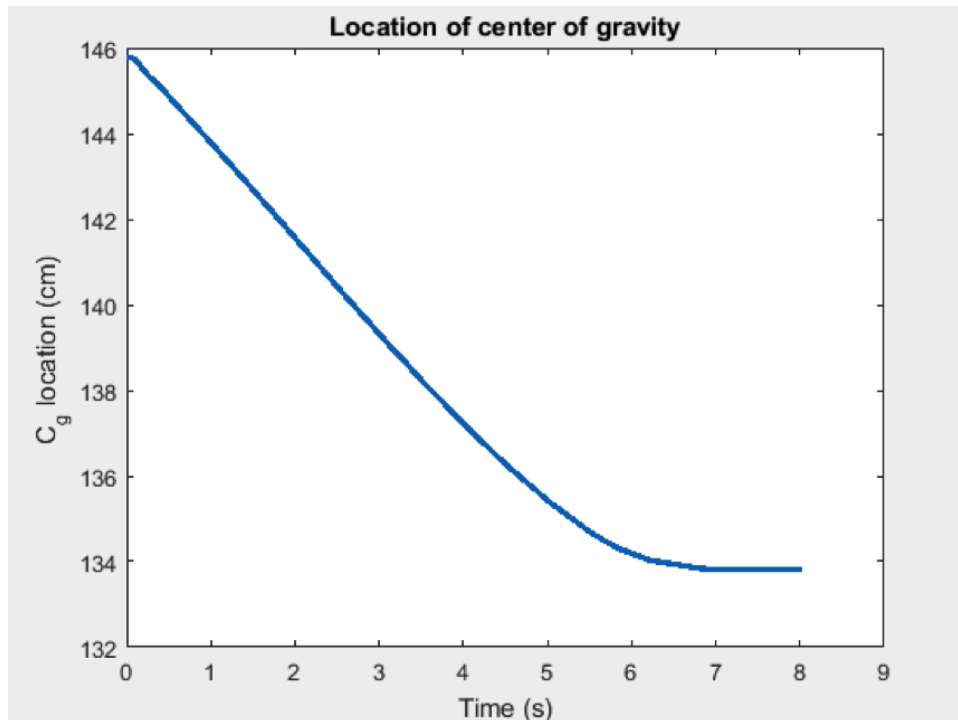


Figure 38: The distance of the center of gravity from the nose of the rocket during flight.

The latter is shown in Figure (44) above. The plot indicates that as the propellant is burned away the mass center of the rocket moves forward toward the nose of the rocket. Throughout the flight, it is important that the center of pressure stay within 1 to 1.5 times the rocket's diameter of the center of gravity. The diameter is 15.6 cm wide. The distance between the center of gravity and center of pressure at the start of the flight is 19 cm, about 1.2 times the diameter. When the motor burns out roughly 7 seconds into the flight, that distance will be twice the diameter. This distance could result in an overly stable rocket that can be made to drift laterally away from the launch pad during flight. This means that the design of the fins, or the weight distribution will have to change to make the distance between the two centers stay within the needed range of the majority of the flight and reduce the lateral drift.

8.3 Failure Analysis

A thorough Failure Modes and Effects Analysis was performed.

Process Function	Part	Potential Failure Mode	Potential Effect(s) of	Mechanism(s) of Failure	Current Process Controls	Recommended Action(s)
Rocket motor burn	Motor Liner	Motor case rupture	Loss of vehicle	Manufacturer defect	Motor assembly process	Ensure proper sealing in place before flight
	Centering rings / thrust structure	Thrust structure failure	Loss of vehicle	Fracture in centering ring, loose screws, or crack	Vehicle assembly process	Ensure proper fitting of fasteners before flight
	Centering rings / thrust structure	Overheating of components	Loss of parachute / damage to vehicle	Excessive thermal environment	Use of insulation to shield vulnerable components	Conduct flight testing and analyze vehicle post-flight
	Vehicle assembly	Errant rocket trajectory	Loss of vehicle	Inherent flight instability	Design process / aerodynamic analysis	Conduct flight testing
Avionics package sensing	Avionics bay	Disruption due to flight forces	Loss of altitude data acquisition, and of parachute deploy capability	Intensive loading	Design process / FEM design methods	Ensure tight fit of the altimeter into the avionics bay
Parachute deployment system	Primary parachute deployment ignition system	Ignition failure / loss of signal from flight computer	Loss of ability to deploy parachute / potential loss of vehicle	Improperly loaded powder grain / intensive loading on	Pre-flight process / design process / FEM design	Ensure that avionics components are secured firmly in
	Main parachute	Failure of parachute to open	Possible loss of vehicle and payload if backup parachute is not	Improper packing method	Vehicle assembly process	Inspect parachute before flight by all team members
	Parachute cord	Breaking of parachute cord	Loss of vehicle and payload	Excessive loading environment / delayed	Design process / faulty avionics software	Redundant shock cord design calculations
	Main parachute	Tear in parachute seams	Possible loss of vehicle and payload if backup parachute is not	Excessive loading environment / delayed	Design process / sewing and stitching work	Conduct flight testing and inspect parachute
Launch sequence	Propulsion ignition mechanism	Failure of mechanism to ignite	Failure to launch immediately	Ignition fuse failure / loss of signal to mechanism	Vehicle launch preparation / wiring of igniton system	Bundle multiple ignition wires
	Flight computer	Failure to send command	Failure to launch immediately	Faulty circuit board / power disconnect	Vehicle launch preparation / wiring of avionics bay	Redundant systems already in place

Figure 39: Failure Modes and Effects Analysis.

9. Project Planning

Team 24 plans to have a design finalized and have orders for components placed by the end of the Fall 2016 semester. A Gantt chart showing the breakdown and dates of tasks for this semester can be found in the Appendix. The work outlined for this project can be broken down into five phases: Background Research and Concept Generation, Detail Design and Analysis, Design Implementation, Test and Revise, and Competition Due Dates.

9.1 Background Research and Concept Generation

This phase consists of detailed background research on rocket motors, fin design, recovery systems, nose cone profiles, potential payloads, and avionics. Background research of the competition was also performed to become more familiar with the competition requirements that our design is to meet. Additionally, this initial stage was used as a time for brainstorming and concept generation for the components required for the rocket and payload.

9.2 Detailed Design and Analysis

This phase was used to select, refine, and analyze our design. Based on the concepts generated during the first phase an initial design was chosen and raw material used for the components were selected. The exact specifications for this design will be refined when an initial CAD model is was, and the model was be updated as the design changed. While the initial CAD model was being developed, a flight control system and recovery system were developed. Once all the components of the initial rocket design are known analysis of the design will begin. The results of the analysis have been used to determine which components of the rocket were in need of being redesigned.. This lead into a tentative final design. An FMEA and H-FMEA were then performed to analyze the potential failure modes of this design. Based on the results of the FMEA and H-FMEA the design required updating. This culminated in into the final design, bill of materials, and cost analysis.

9.3 Design Implementation

Now that the design is finalized, orders will be placed for components of the rocket. Our team will place these orders before the end of the Fall semester.

Currently, Team 24 is intending to order the parts shown in the following table.

Part	QTY
m6x1.25 24mm tap threaded bolt	8
12inch .75inch thickness Aluminum Plate	1
Rail Button set	1
m8x1.25 12mm tap thread bolt	4
3/8in threaded rod	2
m8 bolts package	1
4ft height fiberglass roll (yards)	17
Gallon Epoxy Resin	1
Drop Forged Shoulder Eye Bolt	4
Kevlar Shock Cord (feet)	45
Rocket-Man 3ft Parachute	1
Black Powder	1
Masking Tape Roll	1
3/4 inch plywood plate 1sqft	1
bag of # 2 nylon Shear Pins	1
# 24 Gauge wire (foot)	10
Tenergy Centura Battery	2
TELEGPS Radar Beacon	1
StratoLoggerCF	1
PNUT	1
B2 XXL Parachute	1

Table 8: Bill of materials to be ordered at the end of the fall semester.

More materials will be needed to complete this project, however at this time the materials listed will suffice to build the air-frame .

9.4 Test and Revise

The recovery system, data acquisition, and the experiment will require strenuous ground testing. Additional orders can then be placed if required for better operation of a rocket subsystem. Once all subsystems are performing nominally, a verification launch will be performed, and modifications to the design will be made if necessary.

9.5 Safety and Risks

Given the inherent dangers associated with rocketry and flammable materials in general, it is important that Team 24 take the necessary safety precautions and know the regulations that apply to the activities performed over the course of this project. With this in mind, we contacted the appropriated University staff to open discussion on how the more hazardous aspects of the project were to be handled.

After speaking with Donald Hollett, the Facilities and budget Coordinator at the FAMU-FSU College of Engineering (COE), and Andrew Davis, the Lab Safety Officer in FSUs Environmental, Health & Safety department (EH&S), we found that it was feasible to store the materials in either the Mechanical Engineering Senior Design room or a private storage location on the COE campus, specified by the EH&S department. We intend to follow up on these options with further communication with said parties such that when the purchased materials arrive, the proper storage location will be arranged.

In addition to determining a place for storage Team 24 discussed with EH&S the possibility of performing the deployment test on campus. The deployment test would involve the ignition of black powder charges to demonstrate the separation of the rocket sections. EH&S was open to the idea, so long as a safety plan and risk assessment was drafted, and plans were made for supervision of the test. A detailed safety plan and risk assessment will be submitted to the team's advisors and Donald Hollett and EH&S for review.

At the start of the project there was uncertainty about the regulations associated with transporting hazardous materials. However, the matter of transportation has been largely resolved. Team 24 contacted both the Department of Transportation (DOT) and the Florida Department of Highway safety and Motor Vehicles to determine if there were any regulations that would prevent transporting the materials by private vehicle. There were no exact regulations that either entity could point to that explicitly prohibited this.

9.6 Competition Deadlines

- Project Entry Form
- 1st Progress Update
- 2nd Progress Update
- 3rd Progress Update
- Project Technical Report
- Poster Session Materials
- School Participation Letter
- SAC NMSA Waiver and Release of Liability Form
- SAC ESRA Waiver and Release of Liability Form
- IREC Consent to Limited PII Release Form
- Competition (June 20-24, 2017 in Las Cruces, New Mexico)

Minivan Rental	\$458
Fuel	\$230
7 Nights Hotel Stay	\$900
Total	\$1588

Table 9: Cost breakdown of participating in the competition

9.7 Cost of Participation

Team 24 fully intends to compete at the IREC in Truth-or-Consequences, New Mexico. In order for this to happen Team 24 must procure the funding necessary to go to competition.

Additionally, Team is also responsible for \$900 in competition fees.

10. Conclusion

Sounding rockets have been used for the majority of the last century to further scientific knowledge and engineering goals. It is the aim of Team 24 to continue this by creating a sounding rocket capable of reaching 10,000 ft AGL while performing a scientific or engineering experiment safely. To achieve this goal it is imperative that we focus on the stability, reliability, and avionics package of our rocket. These features will maximize the scientific usefulness of the final product as well as emphasize the importance of safety to this group. Design of the overall system will happen in 4 general steps: pre-design, launch vehicle design, payload integration, and finally, verification and validation. Each of these steps contain the most pertinent requirements to proceed to the next. It is the goal of Team 24 that by completing each step, the final product will be adequate for the competition and provide useful scientific data.

References

- [1] William R. Corliss "NASA Sounding Rockets, 1958-1968 A Historical Summary", Scientific Technical Information Office, 1971
- [2] Gunther Seibert "The History of Sounding Rockets and Their Contribution to European Space Research", European Space Agency, 2006
- [3] Steven Christe and Ben Zeiger and Rob Pfaff and Michael Garcia "Introduction to the Special Issue on Sounding Rockets and Instrumentations", Journey of Astronomical Instrumentation, 2016
- [4] Spaceforest.pl, Demonstrator Rocket, SpaceForest / Demonstrator rocket. [Online]. Available: <http://spaceforest.pl/demonstrator-rocket>. [Accessed: 13-Oct-2016].
- [5] G. A. Crowell, The Descriptive Geometry of Nose Cone, Scribd. [Online]. Available: <https://www.scribd.com/doc/60921375/the-descriptive-geometry-of-nose-cone>. [Accessed: 12-Oct-2016]
- [6] R. L. Norton, Design of Machinery. McGraw-Hill College, 2007. [Accessed: 18-Oct-2016]
- [7] "How rockets work," in Fly Rockets. [Online]. Available: <http://www.flyrockets.com/work.asp>. Accessed: Oct. 11, 2016.
- [8] Y. Gibbs, "X-38 descent with large Steerable Parafoil," NASA, 2015. [Online]. Available: <https://www.nasa.gov/centers/dryden/multimedia/imagegallery/X-38/EC99-44923-102.html>. Accessed: Oct. 11, 2016.
- [9] "Team for advanced flow simulation and modeling," in TAFSM, 2004. [Online]. Available: <http://www.tafsm.org/PROJ/AS/j175STFECCFSIP/>. Accessed: Oct. 11, 2016.
- [10] Peregrine CO2 Ballistic Deployment System Fruity Chutes.
- [11] Overview - Jacobs Rocketry. [Online].
- [12] Subsonic Flow Control - Current Projects. [Online]. Available: <https://aapl.fsu.edu/projects/lpt.html>. [Accessed: 21-Oct-2016].
- [13] CubeSat - Gunter's Space Page. [Online]. Available: http://space.skyrocket.de/doc_sat/cubesat.htm [Accessed: 21-Oct-2016].
- [14] Simulator Data Cesaroni M1450. [Online]. Available: <http://thrustcurve.org> [Accessed: 3-Dec-2016].

- [15] Aluminum Data Sheet. [Online]. Available: <http://arconic.com> [Accessed: 3-Dec-2016].
- [16] COMSOL Multiphysics. [Computer Software]. Available: <http://arconic.com> [Accessed: 3-Dec-2016].

Appendix A

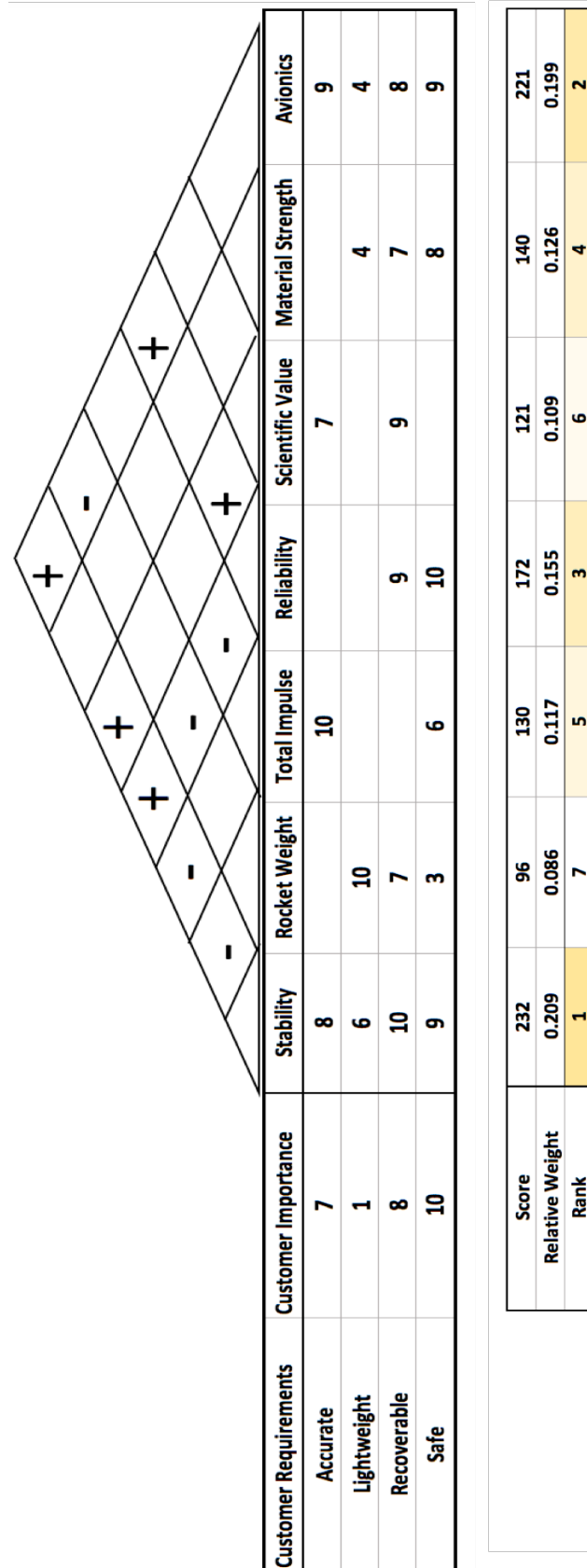


Figure 40: House of Quality comparing Engineering Values with Requirements

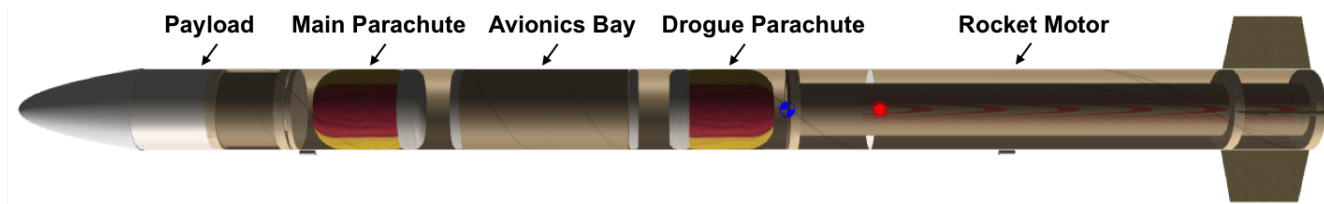


Figure 41: Rocket Subsystems.[4]

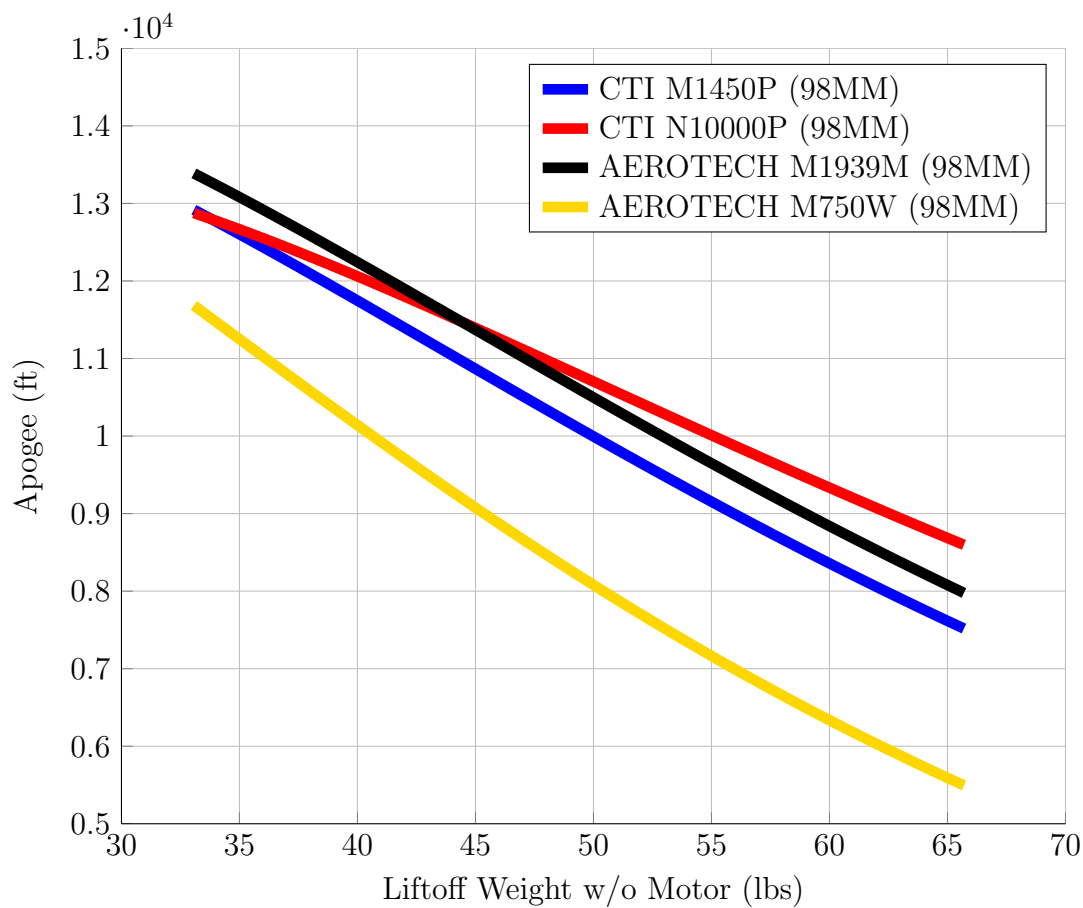


Figure 42: Flight apogees based on mass of rocket for four solid rocket motors.

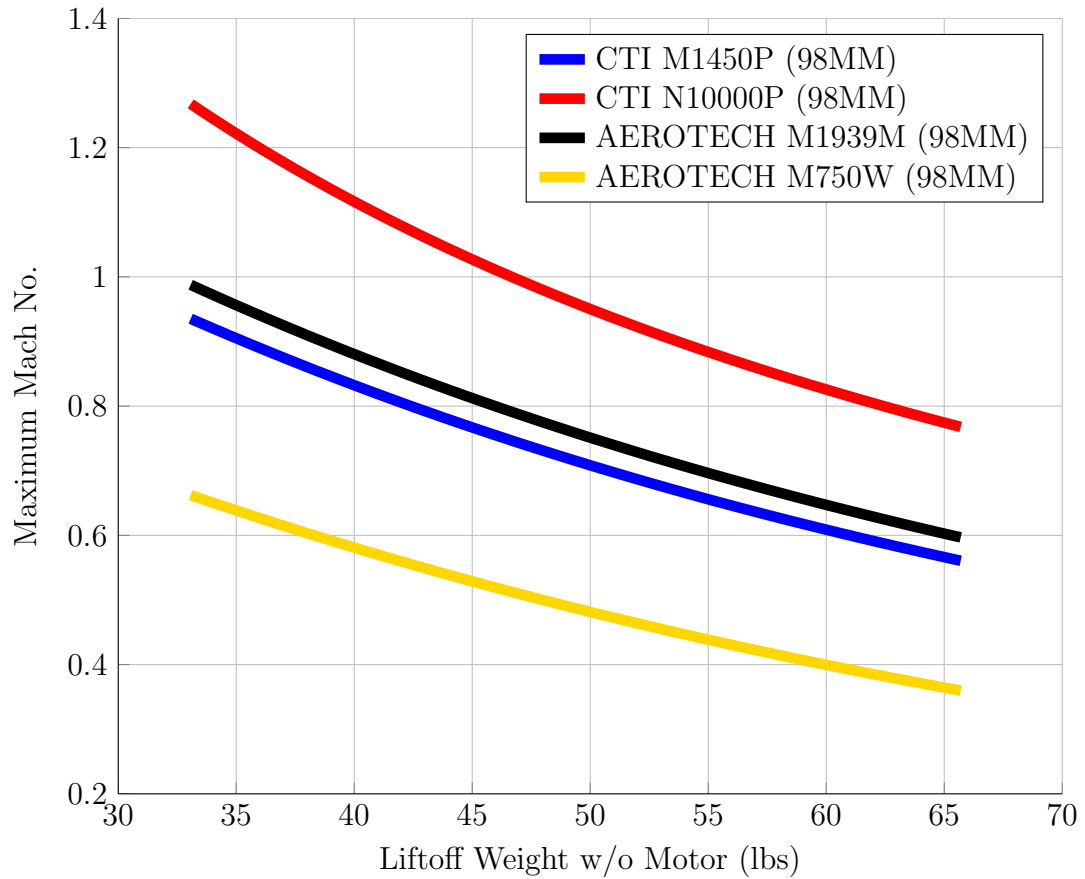


Figure 43: Maximum theoretical mach number based on mass of the rocket for the four different motors analyzed.

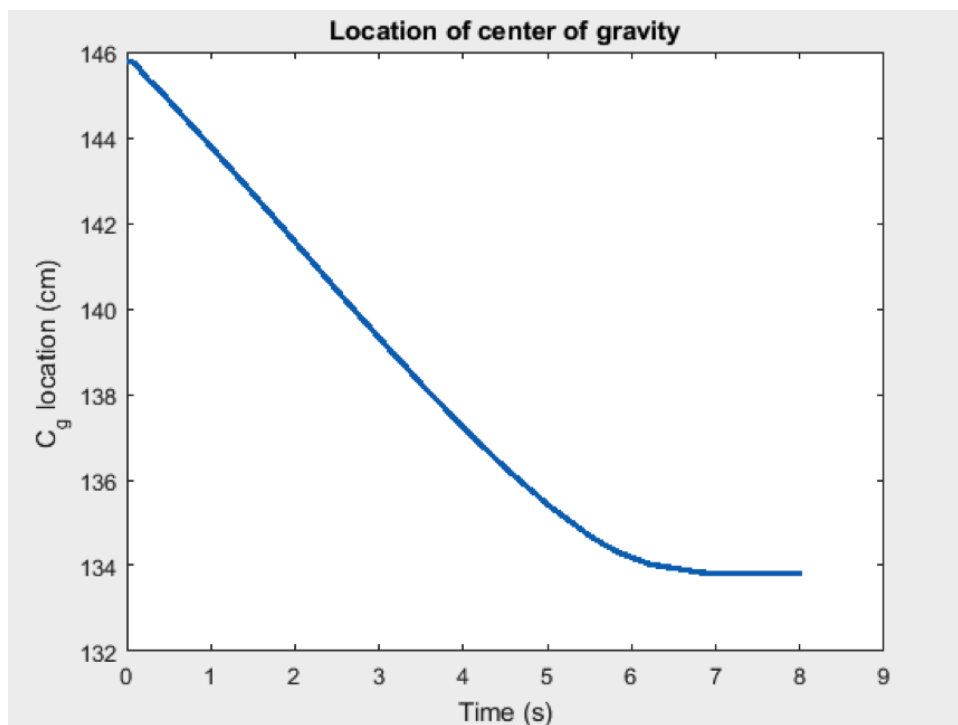


Figure 44: The distance of the center of gravity from the nose of the rocket during flight.

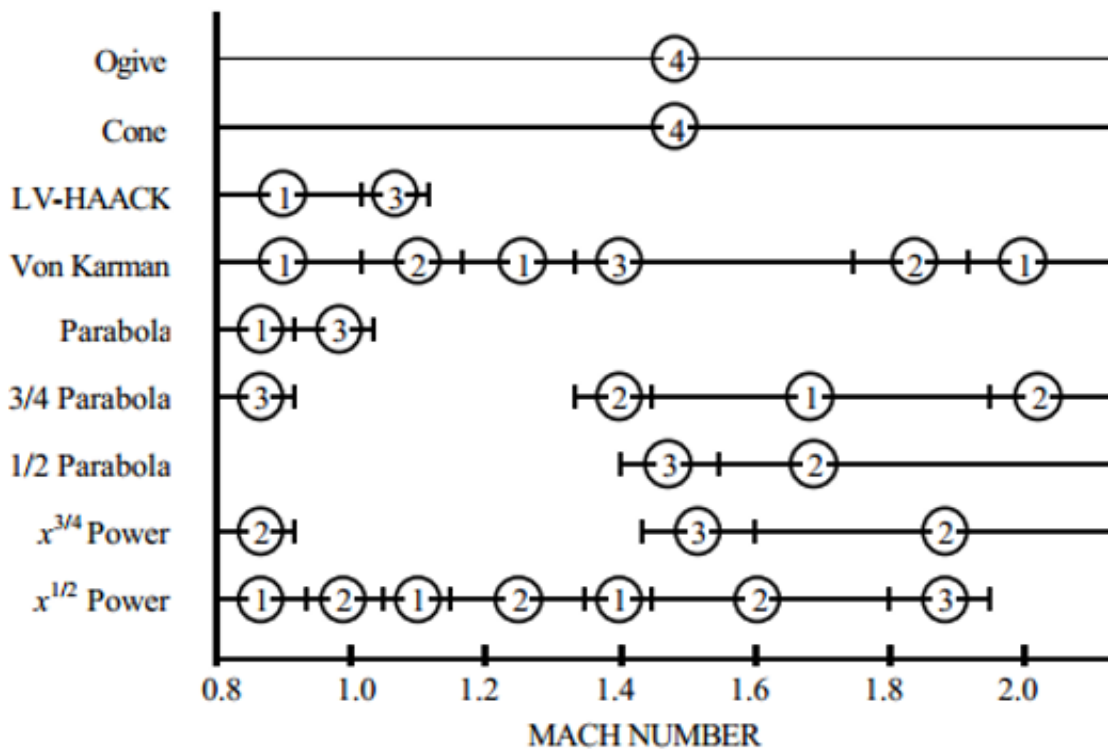


Figure 45: Nose cone profile as a function of mach number.[5]
 1-ideal 2-good 3-acceptable 4-unacceptable

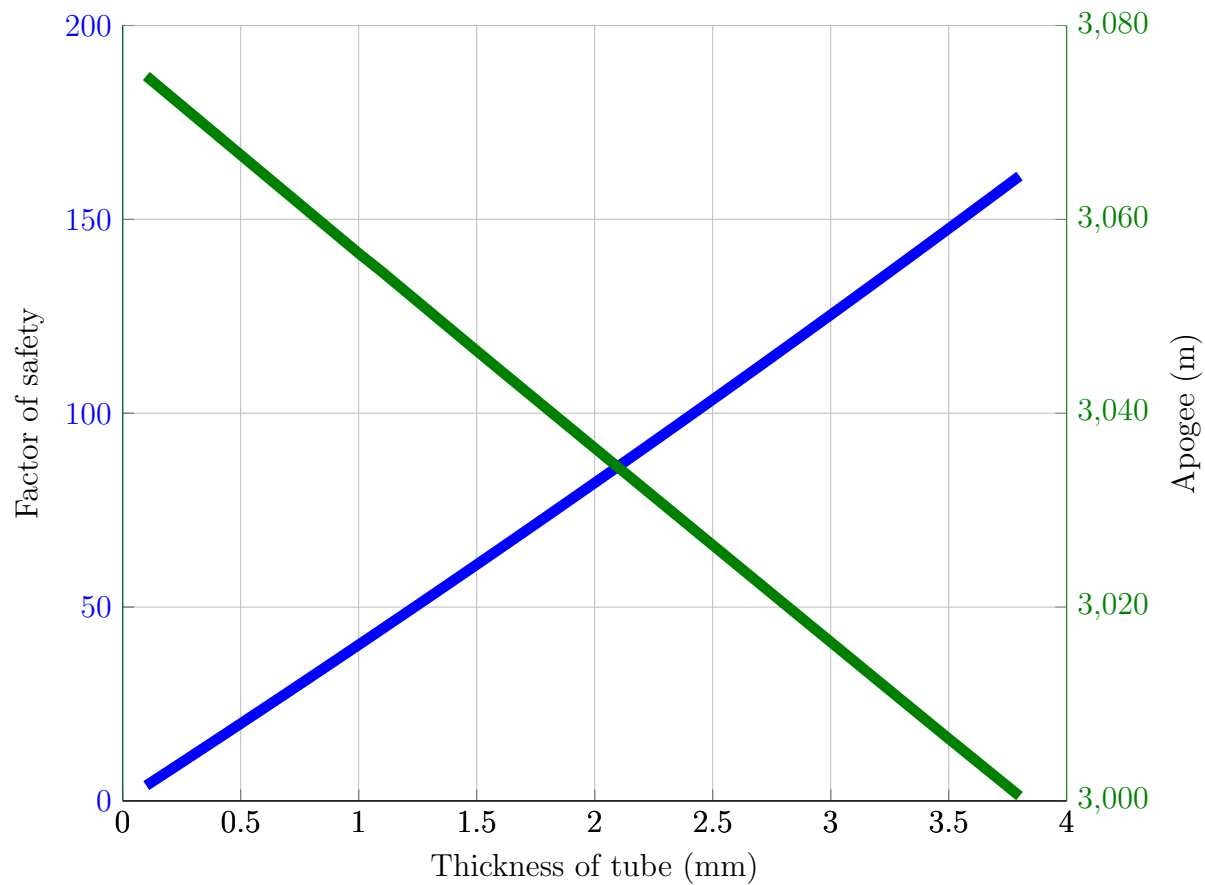


Figure 46: Plot of buckling factor of safety and apogee versus increasing tube thickness.

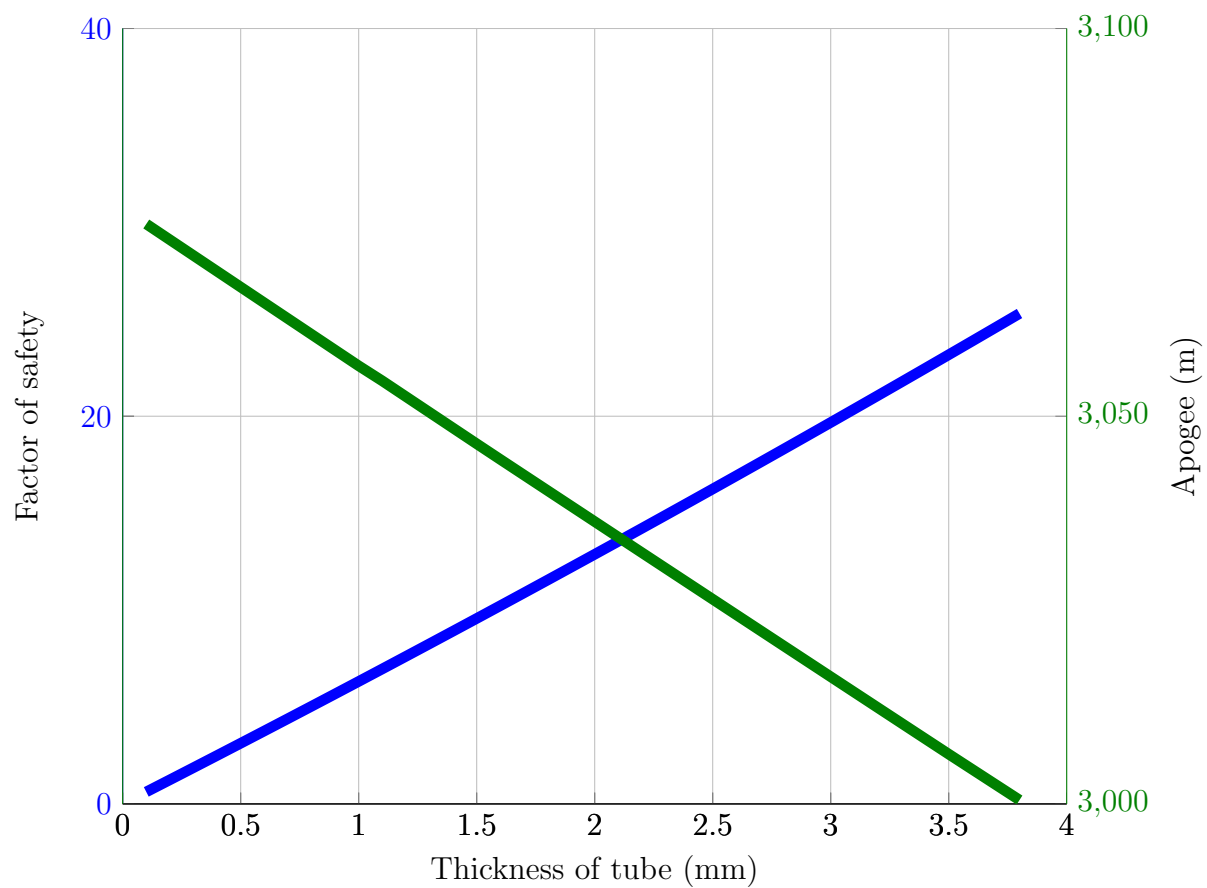


Figure 47: Plot of buckling factor of safety and apogee versus increasing tube thickness using carbon fibre.

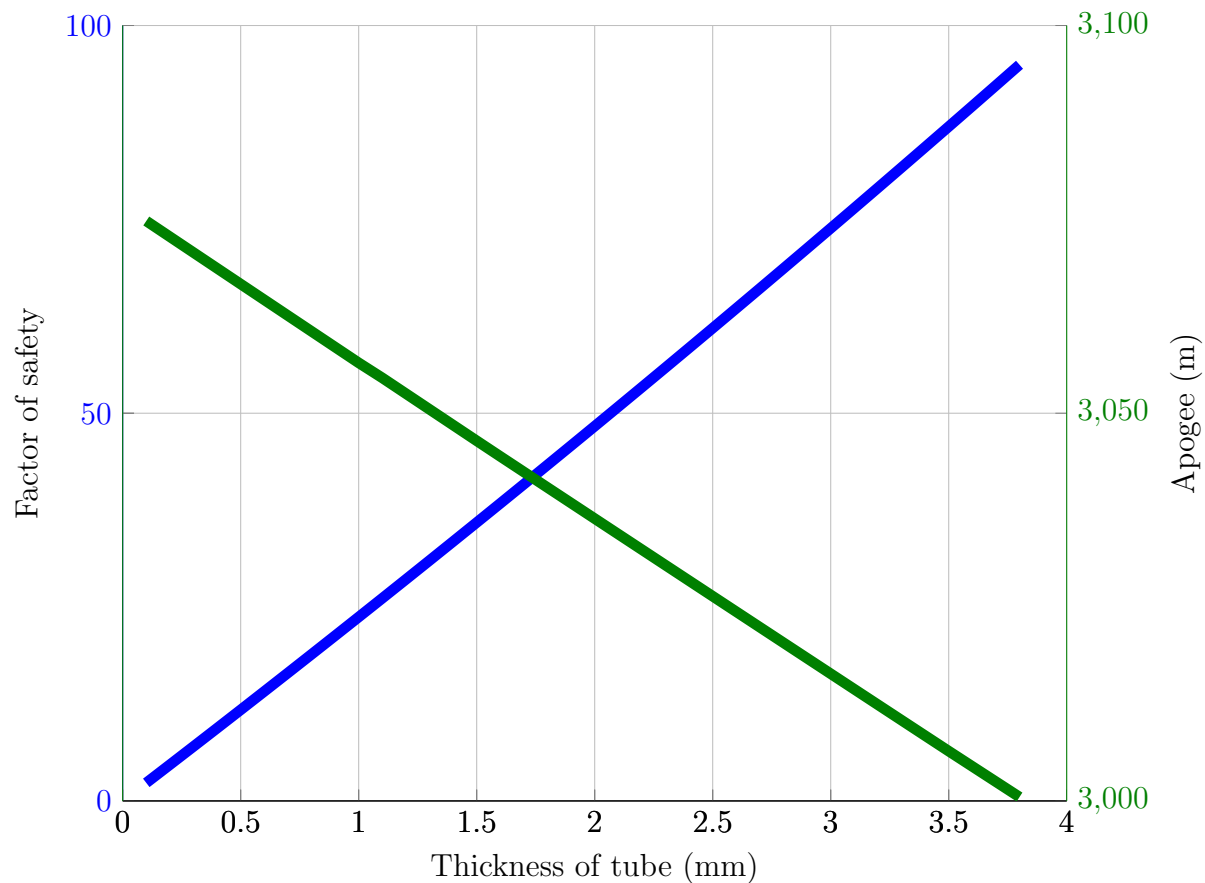


Figure 48: Plot of buckling factor of safety and apogee versus increasing tube thickness using fiberglass.

Engineering Characteristics	Weight	Dual Deployment	Reefed Parachute	Steerable Parafoil
Mass	3	S	+	-
Reliability	3	S	-	-
Cost	2	S	S	-
Range Requirement	3	S	S	+
Complexity	1	S	+	-
Totals		0	1	-6

Figure 49: Pugh Selection Matrix for Recovery System

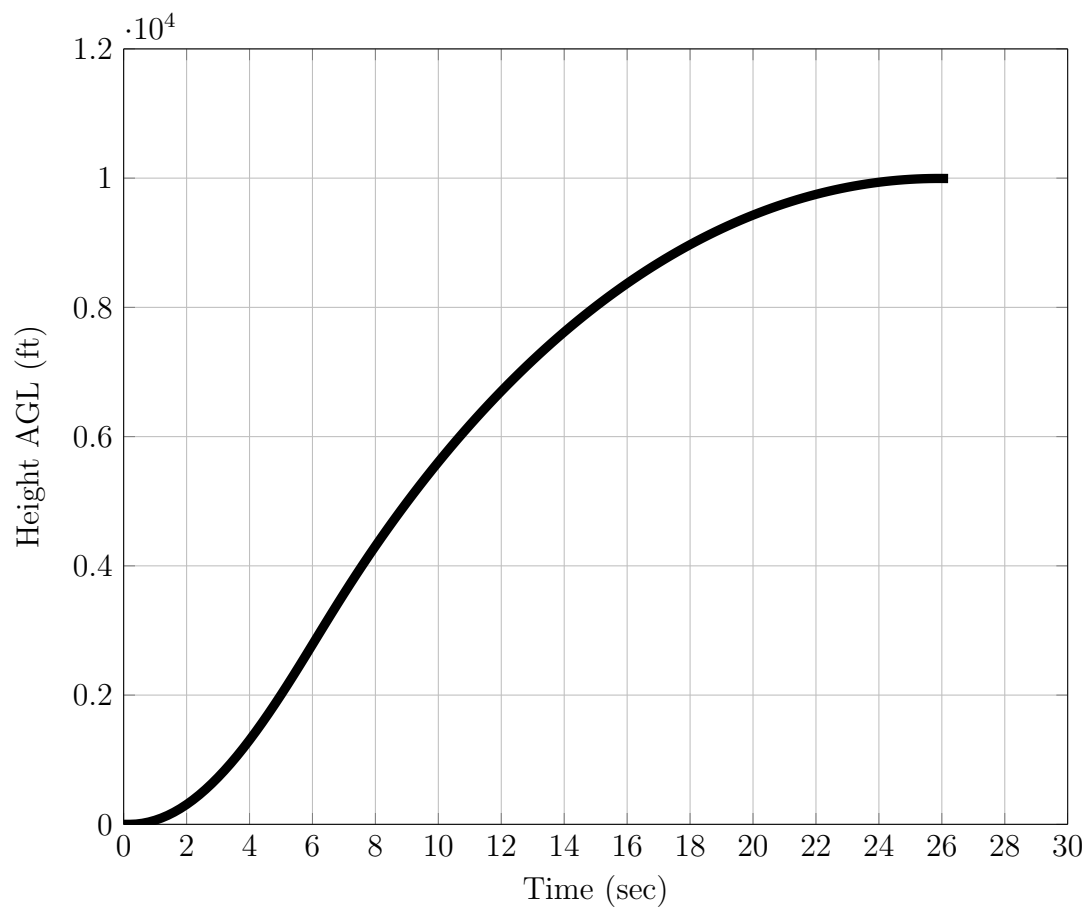


Figure 50: Plot of the height of the rocket AGL during the ascent phase of the flight.

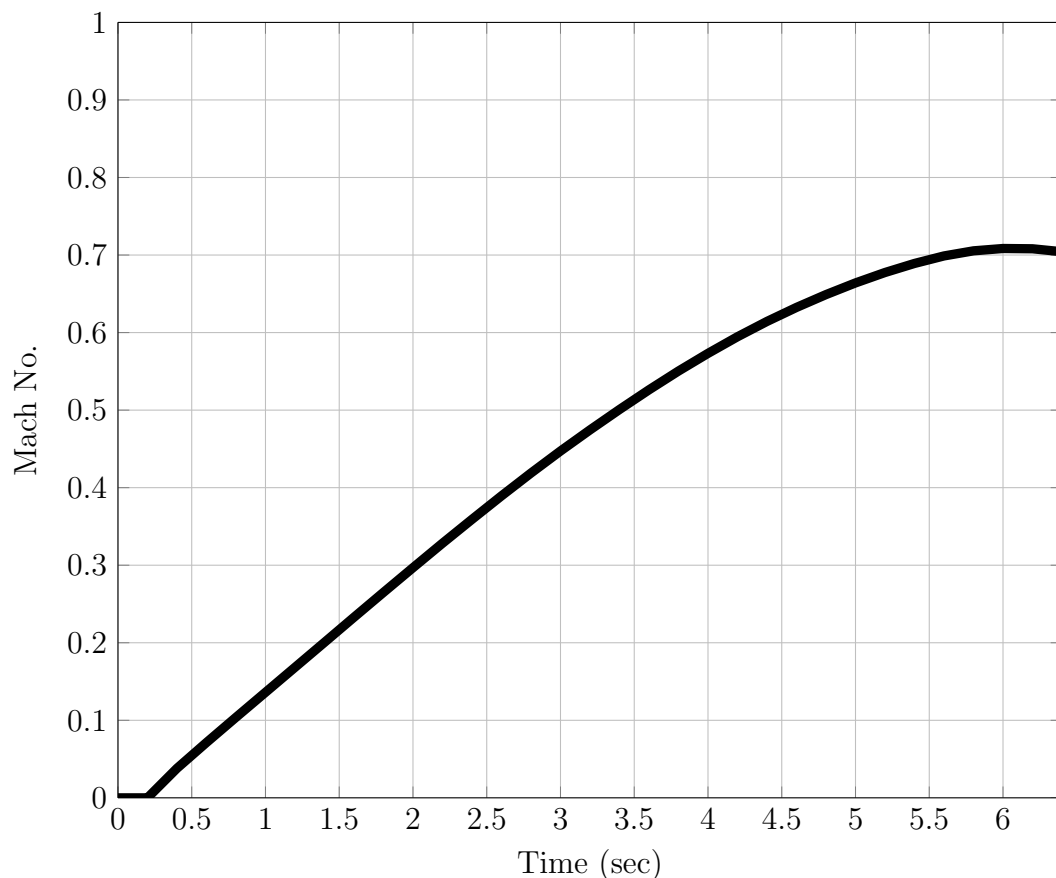


Figure 51: Plot of the mach number of the rocket during the motor burn.

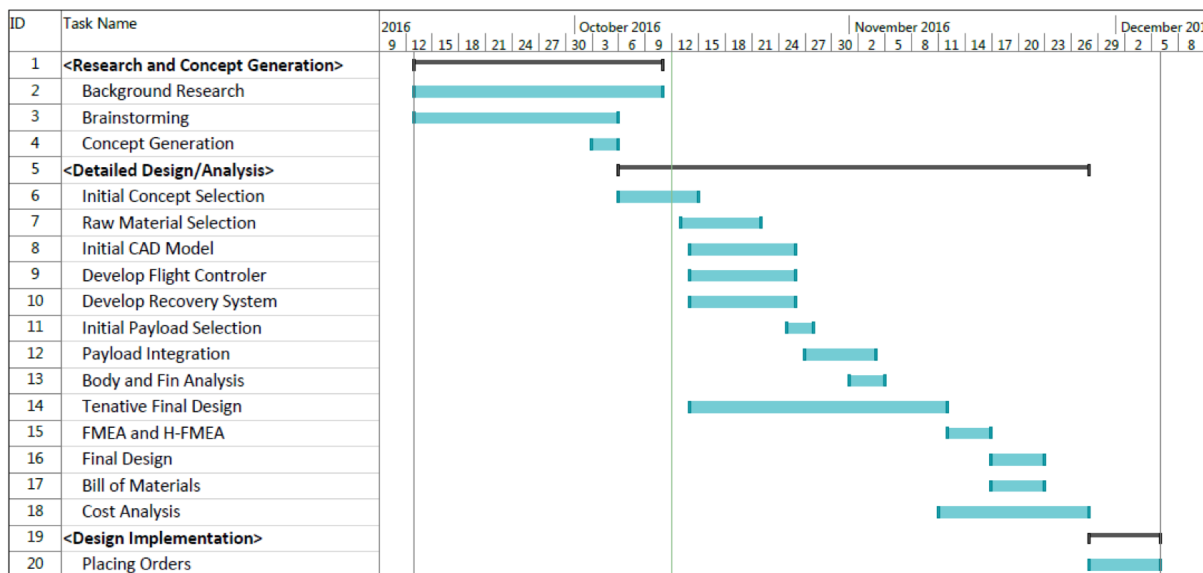


Figure 52: Gantt Chart for Fall 2016

Booster Section	
Component	Cost
M1450 Classic Fuel	\$569.99
M1450 Motor Hardware	\$499.95
M1450 Motor Casing	\$319.95
Fins	\$10.00
Fin Mounting Hardware	\$2.58
Aft Body Tube	\$74.61
Bottom Centering Ring	\$30.00
Fin Centering Ring	\$30.00
Fin Centering Ring	\$30.00
Tube Attachment Hardware	\$2.00
Top Centering Ring	\$30.00
Threaded Rods	\$6

Table 10: Booster Section Cost. Each component is listed by its location within the section from bottom to top.

Drogue Parachute Section	
Component	Cost
Drop Forged Shoulder Eye Bolt	\$12.96
Kevlar Shock Cord	\$14.55
Rail Button	\$5.00
Rocket-Man 3ft Parachute	\$35.00
Drop Forged Shoulder Eye Bolt	\$12.96
Drogue Section Tube	\$37.30

Table 11: Drogue Section Cost. Each component is listed by its location within the section from bottom to top.

Avionics Bay	
Component	Cost
Black Powder Container	\$6.00
Black Powder Charge	\$8.00
Plywood Avionics End Cap	\$13.48
Outer Avionics Body	\$21.44
Threaded 3/8 inch Rod	\$8.00
# 2 Nylon Shear Pins	\$10.00
ABS Avionics Mounting Board	\$2.00
# 24 Gauge Wiring	\$83.50
Tenergy Centura Batteries	\$13.50
TELEGPS Radar Beacon	\$214.00
StratoLoggerCF Flight Computer	\$54.95
PNut Flight Computer	\$55.95
Plywood Avionics End Cap	\$13.48
Black Powder Container	\$6.00
Black Powder Charge	\$8.00

Table 12: Avionics Bay Cost. Each component is listed by its location within the section from bottom to top.

Main Parachute Bay	
Component	Cost
Drop Forged Shoulder Eye Bolt	\$12.96
Main Parachute Bay Tube	\$27.97
Kevlar Shock Cord	\$29.10
B2 XXL Parachute	\$239.00
Drop Forged Shoulder Eye Bolt	\$12.96

Table 13: Main Parachute Bay Cost. Each component is listed by its location within the section from bottom to top.

Nose Cone	
Component	Cost
Nose Cone Bodyu	\$27.97
Upper Rail Button	\$5.00
Cubesat Payload Container	Unknown
Payload Mounting Rings	\$2.00
Printed Nose Cone	\$3.00

Table 14: Nose Cone section Cost. Each component is listed by its location within the section from bottom to top.

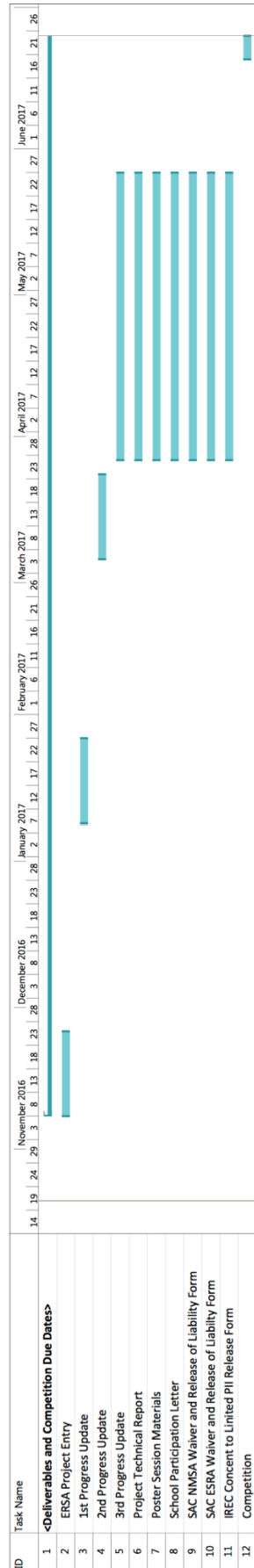
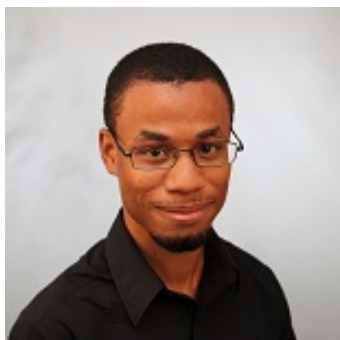


Figure 53: Gantt Chart for Competition Deadlines

Biography



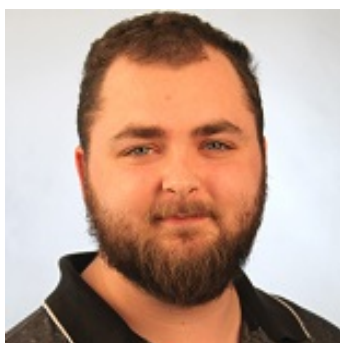
Tariq Grant is a Florida State University student in his senior year of Mechanical Engineering. He is currently a research volunteer at the Center for Intelligent Systems, Controls, and Robotics. Tariq is also the President of the American Institute of Aeronautics and Astronautics student organization at the FAMU-FSU College of Engineering.



Alex Mire is a Florida State University Mechanical Engineering student. For the past two summers, she has had summer internships with Jacobs Technology in the Kennedy Space Center. She is a member of the American Society of Mechanical Engineers and FSU's Flying High Circus.



Brandon Gusto is a double major in mechanical engineering and applied mathematics at FSU. He is interested in the development of computational fluid dynamics algorithms in the field of aerospace engineering. He spent his most recent summer at the Los Alamos National Laboratory where he worked on parallelizing shock hydrodynamics codes.



William Pohle is a senior Mechanical Engineering student at the FAMU-FSU College Of Engineering. He spent his last summer in Indiana working for Norfolk Southern resolving repair issues and train derailments. Previously William has volunteered his time at the High Performance Materials Institute in Tallahassee where he helped develop a new composite material.